THE PENNSYLVANIA STATE UNIVERSITY
SCHREYER HONORS COLLEGE

DEPARTMENT OF BIOCHEMISTRY AND MOLECULAR BIOLOGY

EFFECT OF THE GOLGI ON DROSOPHILA DENDRITIC MICROTUBULE NUCLEATION

CHRISTIE J. MCCRACKEN

Spring 2010

A thesis
submitted in partial fulfillment
of the requirements
for a baccalaureate degree
in Biochemistry and Molecular Biology
with honors in Biochemistry and Molecular Biology

Reviewed and approved* by the following:

Melissa M. Rolls
Assistant Professor of Biochemistry and Molecular Biology
Thesis Supervisor

Chen-Pei David Tu
Professor of Biochemistry and Molecular Biology
Honors Adviser

Scott B. Selleck, Department Head
Department of Biochemistry and Molecular Biology

* Signatures are on file in the Schreyer Honors College

Abstract

Microtubule arrays are best studied during mitosis, at which time the centrosome nucleates the minus ends of microtubules while the plus ends grow out in a radial array. Contrary to this model, fully differentiated *Drosophila* cells, including neurons, do not contain centrosomes (Rogers et al., 2008), so they must use some other means of microtubule nucleation. It has been shown in various cell types that the Golgi apparatus can nucleate microtubules independently of the centrosome (Efimov et al., 2007). Golgi outposts have also been found in neuronal *Drosophila* dendrites (Ye et al., 2007), a region in which most microtubules are oriented with minus ends directed distally from the cell body. Thus, it has been proposed that Golgi could be nucleating microtubules in *Drosophila* dendrites. In order to test this hypothesis, I cloned a kinesin/Golgi fusion protein into fly lines with the assumption that the fusion would pull Golgi out of the dendrites (towards microtubule plus ends). Based on antibody staining, several of the fly lines were shown to be expressing the fusion proteins in larvae. These fusions moved about half of the Golgi outposts out of the dendrites and some Golgi into axons, as was seen using fluorescence microscopy to image class IV dendritic arborization (da) neurons. However, imaging Golgi in wild type class I da neurons revealed very few Golgi in the dendrites. This lack of dendritic Golgi in the class I da neurons makes the Golgi an unlikely candidate for nucleating microtubules in dendrites. This inference was supported by analyzing microtubule dynamics using lava lamp (lva) RNAi to knock down Golgi function in the dendrites. In these neurons, microtubule dynamics remained very similar to control neurons. So far, dendritic Golgi outposts show no evidence of being microtubule nucleation sites. However, it would still be interesting to further investigate the kinesin/Golgi fusion lines and their phenotypes in dendrites and axons.

TABLE OF CONTENTS

Introduction 1

Materials and Methods 11

Chapter 1: Are the fusions being expressed? 25

Chapter 2: What can I use to best visualize the Golgi? 35

Chapter 3: Where do I see Golgi localized in the fusion lines? 40

Chapter 4: What can I discover using an alternate method to deplete the Golgi? 53

Conclusions 58

References 59

INTRODUCTION

Neuron background (function, structure, and signaling):

Our bodies contain vast networks of neurons that allow communication with the brain. Neurons quickly transfer electrochemical signals throughout the body, which is how the brain obtains all of its information. Damage to neurons causes serious health problems because this system is essential for proper communication within the body. This is why neurological diseases can be so debilitating and why so much time is being spent researching these diseases. Some of them are caused by problems in development of the nervous system, while others are degenerative diseases. In humans, some of the most common neurological diseases include Alzheimer's, Creutzfeldt-Jakob Disease, Epilepsy, Huntington's Disease, and Parkinson's Disease. These diseases are still in the process of being fully understood as scientists come to better comprehend neuronal function and development.

Although there are several different types of neurons, they all have the same general structure. Each neuron consists of at least one axon and multiple dendrites which extend from the soma, the cell body of the neuron. The dendrites are generally post-synaptic processes where signals are received, while the axon is the pre-synaptic process where signals are transmitted on to another cell. Because of these processes with their specific functions, neurons are highly polarized cells. Dendrites and axons require different molecules to equip them to either receive or transmit a signal through the synapse. It appears that the corresponding molecules are specifically transported into either the axons or dendrites since researchers can see different proteins specifically localized to a certain portion of the neuron (Craig and Banker, 1994; Conde and Caceras, 2009).

The process of neuronal signaling is quite complex. The neuron transfers an intracellular electrical signal from its dendrites to its axon. However, the cell transmits an intercellular chemical signal through the synapse from the axon to the dendrites of the next neuron. This synaptic signal requires various neurotransmitters to be present in the axon terminal, where they are conveyed through synaptic vesicles into the synaptic cleft to pass the signal to the dendritic tips. The neurotransmitters bind to specific receptors on the dendritic side of the synaptic cleft and begin signal cascades. Thus, different neurotransmitters send different signals to the neuron. These neurotransmitters are produced in the soma and transported out the axon to the synapse. In order to activate the passage of neurotransmitters through the synapse, there must also be calcium channels out in the tip of the axon. These calcium channels are activated to take up calcium by the change in membrane potential as the electric signal from the dendrites reaches the axons. The higher calcium levels initiate the release of neurotransmitters from synaptic vesicles into the synaptic cleft to pass the signal to the next cell. Thus, this complex machinery must function coordinately throughout the neuron in order to transmit signals properly (Rothwell, 2009).

Neuronal processes:

Along with their divergence of function, axons and dendrites are morphologically different. They vary both structurally and in the molecules that localize to the different processes. As dendrites extend out from the cell body and branch, the diameter of the processes decreases so that the total cross-sectional area remains about the same. However, the cross-sectional area of some axons can increase as they get farther from the soma or when they divide at branch points (Craig and Banker, 1994; Arimura and Kaibuchi, 2007). It has also been known for a long time that there are molecules that localize specifically to either dendrites or axons. An early report of this by Matus et al. showed that certain “high molecular weight microtubule-associated proteins” that promoted microtubule polymerization only localized to dendritic microtubules of neurons (1981). Some specific molecules were characterized for neuronal localization by Rolls et al. (2007). These included nod, which localized to dendrites, and tau, which localized mainly to axons. Another protein, Apc2, was seen to localize to the cell bodies, dendrites, and the proximal region of axons but not the main branch of the axon. According to Adams et al., the sodium ion channel protein pickpocket localized mostly to the soma and slightly to the dendrites, but not to the axons (1998). These are only a few of the molecules that localize to a specific region within neurons.

***Drosophila* as a model system:**

Drosophila melanogaster has long been used as a model system for research. Flies are easy to manipulate genetically and have short generation times. They also can provide a system for *in vivo* research that complements the more abundant research of cultured neurons. This is a powerful tool for the researcher who wants to observe the effects of differentiation signals and other regulatory signals that the neurons receive *in vivo*. The Rolls lab mainly looks at *Drosophila* dendritic arborization (da) neurons, which are sensory neurons located on the periphery of the flies. Because they are just under the larval cuticle, the da neurons are easy to image using a confocal microscope.

Microtubules:

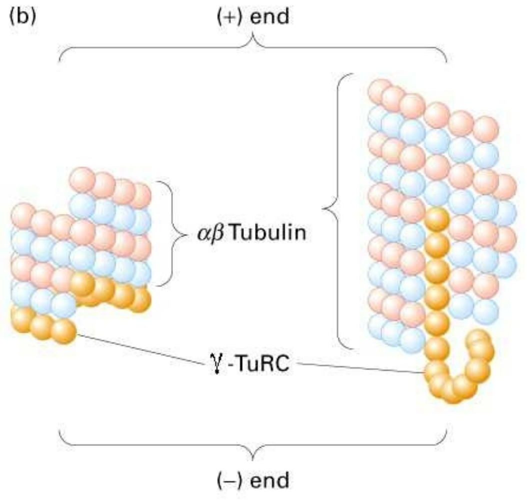

Figure 1: γ-tubulin and γ-TuRC anchor the minus end of the microtubule.

http://bioweb.wku.edu/courses/biol22000/29Microtubules/images/F19-08B.JPG

Neurons must be able to transport proteins, ion channels, neurotransmitters, and many other molecules over a long distance from the cell body to a neuronal synapse. In order to do this, the cell uses a network of microtubules throughout the axons and dendrites. Microtubules are part of the cytoskeleton and are used in most cells for transport. They are long, hollow polymers mainly composed of α- and ß-tubulin. Another form of tubulin, γ-tubulin, forms the first layer of tubulin at the base of the microtubule and acts as an anchor from which the microtubule can grow. It is found along with other proteins in γ-tubulin ring complexes (γTuRC), from which microtubules are seen to grow (Figure 1).

The sites of microtubule nucleation containing γTuRC are called microtubule organizing centers (MTOCs). The most well known MTOC is the centrosome. During nucleation to form microtubules, α- and ß-tubulin monomers join to form heterodimers. The tubulin dimers then bind in the same orientation to form oligomers such that the tubulin subunits always alternate. These oligomers join together in a hollow circle that contains thirteen units of tubulin around its circumference. Each longitudinal filament of tubulin making up the microtubule is called a protofilament (Figure 2). Once the microtubule is formed, it is dynamic, meaning that it can still grow or retract (depolymerize), as shown in Figure 3. This is regulated by GTP hydrolysis. Two GTP molecules are bound to each tubulin heterodimer. The GTP on the α-tubulin subunit is stable but the GTP on the ß-tubulin can be hydrolyzed. When the tubulin heterodimers bind to the tip of the microtubule, the GTP bound to the ß-tubulin can be hydrolyzed to GDP, which makes it prone to

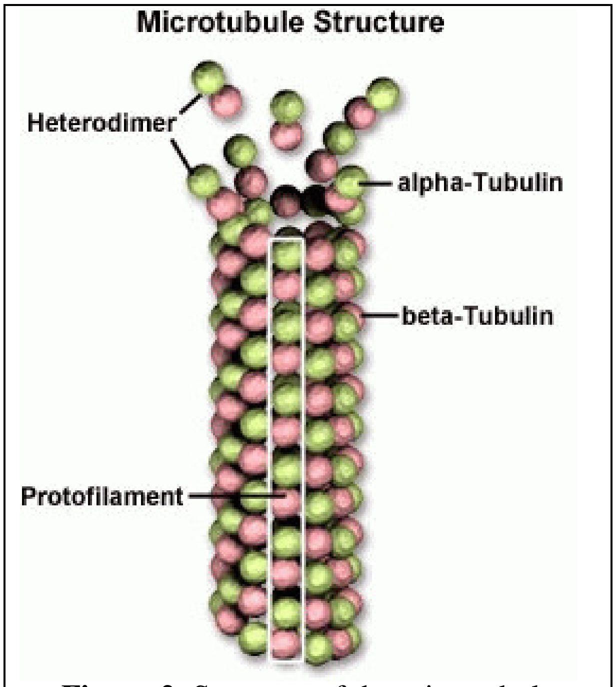
Microtubule Structure
Heterodimer
alpha-Tubulin
beta-Tubulin
Protofilament

Figure 2: Structure of the microtubule showing heterodimers of α- and ß-tubulin.

http://vbaulin.front.ru/research/images/microtubule.gif

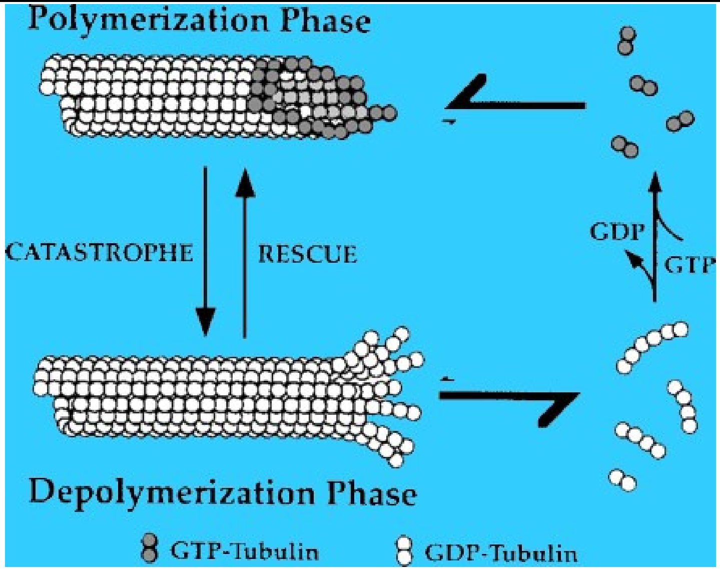
Polymerization Phase
CATASTROPHE
RESCUE
GDP
GTP
Depolymerization Phase
GTP-Tubulin
GDP-Tubulin

Figure 3: Microtubules growing and depolymerizing

http://www.wadsworth.org/bms/SCBlinks/mcewen/Media/fig_3_micro_tub_dyn_inst_3.jpg depolymerization. The GDP-bound tubulin is unstable and will more easily fall off the end of the microtubule than GTP-bound tubulin (Mitchison and Kirschner, 1984). However, if there is a lot of tubulin being added to the microtubule at once, it will form a "cap" which will keep the microtubule from depolymerizing because hydrolysis to GDP will be unable to keep up. Microtubule-associated proteins (MAPs) bind to microtubules and help to stabilize them or cross-link them to other structures in the cell. Because tubulin dimers always assemble in the same orientation, one end of the microtubule will have free α-tubulin subunits and the other will have free ß-tubulin subunits. The end with the exposed ß-tubulin is designated the plus end, while the end with the exposed α-tubulin is designated the minus end. This makes microtubules polarized, and motors that transport cargo along microtubules can only move in one direction towards either the plus end or the minus end.

Microtubule organizing centers:

In the standard cell, the microtubule array is anchored at the centrosome (Figure 4). Microtubule minus ends are nucleated with γ-tubulin into a ring complex near the centrosome and the plus ends extend from there. The classic microtubule array resembles an aster and is distributed equally in all directions from the centrosome. The plus ends generally grow out to the edges

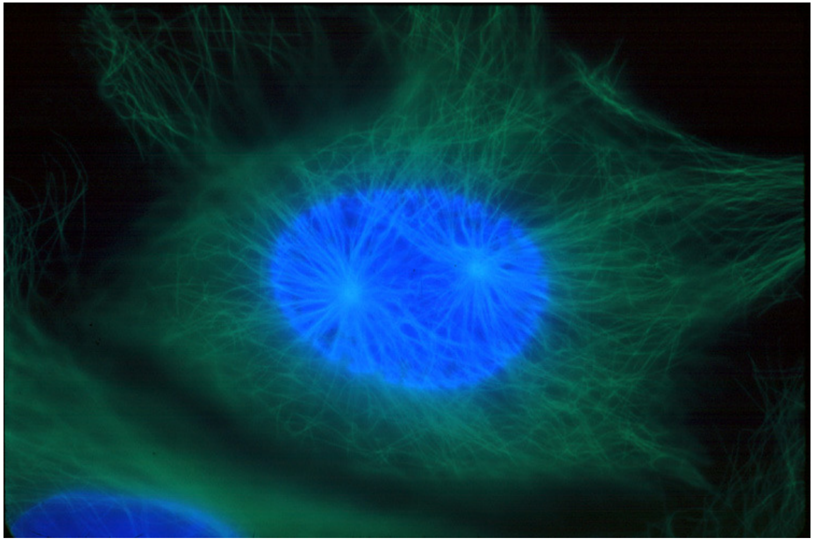

Figure 4: Microtubule arrays nucleated at two centrosomes during prophase

http://www.wadsworth.org/bms/SCBlinks/web_mit2/RES_MIT.htg/imf1.jpg of the cell so that cargo can be transported throughout the cell. Microtubules can also grow towards one end of the cell and thus help in moving a cell or changing its shape. However, this model presupposes that a microtubule can grow long enough to reach the edge of the cell. In neurons, microtubules must extend through axons and dendrites to the synapses. For most neurons, this is a much greater distance than can be reached by a single microtubule nucleated in the cell body. This presents a question of how the microtubules are nucleated. One popular model is that microtubules grow from the centrosome and are then severed by proteins such as katanin and transported out into the neurites (Baas et al., 1993; Ahmad et al., 1999; Baas et al., 2005). This would suggest that microtubules must originate from the centrosome. Then they would be separated from the centrosome but continue to exhibit dynamic instability from the plus end as long as the entire microtubule did not depolymerize. This assumes that the microtubules need no nucleation site once they first grow. Research in *Drosophila* has presented a unique situation. There are no functional centrosomes during interphase in certain *Drosophila* cell types including neurons (Rogers et al., 2008). Fly centrioles seem to completely lack pericentriolar material components, which compose part of the centrosome surrounding the centrioles, during interphase (Rogers et al., 2008). Therefore, microtubules cannot be nucleated at centrosomes in *Drosophila*.

In looking at microtubule nucleation and arrangement in neurons, it is helpful to consider microtubule polarity. The first studies of microtubule polarity involved the hook method, where exogenous tubulin is incubated with *in situ* cells that are then lysed. This tubulin will polymerize and form curved sheets that bind to the microtubules from the cells. When the microtubules are cut in cross sections and visualized using electron microscopy, the exogenous tubulin appears as hooks that curve a certain direction depending on the polarity of the microtubule (McIntosh and

Euteneuer, 1984). If the hook curves clockwise, this indicates that the plus-end of the microtubule is directed out of the tissue sample towards the eye when looking at it on the microscope, and if the hook curves counterclockwise, the microtubule minus-end is oriented toward the eye. This hook method has been used to evaluate microtubule polarity in axons of many neurons, including cultured rat hippocampal neurons (Baas et al., 1988) and frog olfactory neurons (Burton and Paige, 1981). In all of the neurons that have been analyzed, from both the peripheral and central nervous systems, it has been found that at least 95% of axonal microtubules were oriented in the same direction. Dendritic microtubules have been studied much less, but several studies did assay microtubule polarity in dendrites as well. In rat hippocampal neurons, proximal dendrites were found to contain mixed orientation microtubule arrays, while the more distal dendrites contained a higher proportion of plus-end out microtubules (Baas et al., 1988). However, a recent study used second-harmonic generation from microtubules to examine microtubule polarity in *in vivo* mouse neurons and found a polarized dendritic microtubule array in pyramidal neurons rather than the expected mixed orientation (Kwan et al., 2008). This method does not differentiate between microtubule orientation, so it cannot be determined whether the microtubules were plus-end out or minus-end out. In addition to the hook method and second-harmonic generation, microtubule polarity can also be determined using fluorescence microscopy *in vivo* to follow microtubule plus-end binding proteins. This shows the direction in which the microtubule plus end is growing. This method has been used in *Drosophila* to look at microtubule polarity in several types of *Drosophila* neurons. This analysis revealed that the axonal microtubule polarity was plus-end out, as seen previously in vertebrate neurons. However, the proximal dendritic microtubules were seen to be about 90% minus-end out instead of the mixed orientation found in vertebrates.

In distal dendritic branches, microtubules had a more mixed orientation (Stone et al., 2008). This is very interesting because it shows a different orientation of microtubules in *Drosophila* than what has been considered standard for mammalian neurons. The variation could arise from the fact that these neurons are found in invertebrates or that they were assayed *in vivo*, which represents a different environment from the *in vitro* neurons previously assayed.

Since dendrites, especially in *Drosophila* neurons, contain more minus-end out microtubules than axons, the question of microtubule nucleation becomes even more interesting. Assuming that microtubule minus ends must be nucleated in some sort of MTOC, a minus-end out microtubule array in dendrites necessitates that there is some MTOC located out in the dendrites. When considering possible nucleation sites, it is helpful to first look at what can actually be found in the dendrites. Most organelles are found in the neuronal cell bodies but may not be found in the processes. Examples of organelles found in both axons and dendrites are mitochondria and vesicles. There are also several organelles found exclusively in dendrites but not axons, which would be good possibilities for nucleating microtubules in the dendrites. These include rough endoplasmic reticulum, Golgi bodies, and neurotransmitter receptors (Stone et al., 2008). Also, early endosomes seem to be excluded from axons but frequently found in dendrites (Parton et al., 1992). Since none of these are found in axons, it makes sense that they could be needed in the dendrites to nucleate the microtubule minus ends while not needed in axons. Another factor to consider is whether or not these organelles can nucleate microtubules. It has been shown that the Golgi complex can nucleate a fraction of microtubules in many cell types independently of centrosomes (Efimov et al., 2007). It has also been well-documented that there are Golgi outposts in dendrites (Ye et al., 2007). Therefore, I hypothesize that the Golgi apparatus is nucleating microtubules in dendrites.

Golgi bodies:

Golgi bodies are part of the secretory system and are responsible for processing proteins made in the cell. The Golgi receives proteins made in the rough endoplasmic reticulum and is involved in modifying and folding these proteins before transporting them to their destination either inside or outside the cell. Proteins destined to be transported out of the cell are packaged into vesicles that bud off of the trans face of the Golgi and travel to the plasma membrane, where they fuse with the membrane, releasing their contents to the outside. Along with proteins, the Golgi can also transport lipids around the cell. Additionally, it creates lysosomes by transporting hydrolytic enzymes to early endosomes. In most cells, the full Golgi apparatus sits near the endoplasmic reticulum. However, in invertebrates, including *Drosophila*, the Golgi is divided into many puncta. In neurons, the Golgi serve an important role since so many molecules need to be synthesized and transported out to the synapses. In both mammalian (Horton et al., 2005) and *Drosophila* neurons (Ye et al., 2007), it has been found that there are Golgi outposts in the dendrites. Thus, I will test whether the Golgi might be nucleating microtubules in *Drosophila* da neuron dendrites using a kinesin-Golgi fusion to pull the Golgi out of the dendrites.

MATERIALS AND METHODS

Plasmid Construction:

In order to evaluate the effects of removing the Golgi from the dendrites, three kinesin/Golgi fusions were obtained from Sean Munro at the MRC Laboratory of Molecular Biology, Cambridge (called GRIPs 22, 26, and 38). Each fusion contained the rat kinesin domain Kif5b (or KHC), which is the heavy chain of kinesin (Brady, 1985). This gene is homologous to many other species including mice, humans, and *Drosophila*. The Golgi domains differed between the three fusions, with GRIP22 containing the C-terminus region of the cis Golgi protein GMAP210, GRIP26 containing the C-terminus of the trans Golgi protein golgin-97, and GRIP38 containing no Golgi domain to serve as a negative control. The kinesin and Golgi domains were connected with a linker and myc tag (Figure 5). Since these fusions were given to me in mammalian vectors, they were cloned out of the vectors and into the fly vector pUAST 3YCT, which was then injected into embryos.

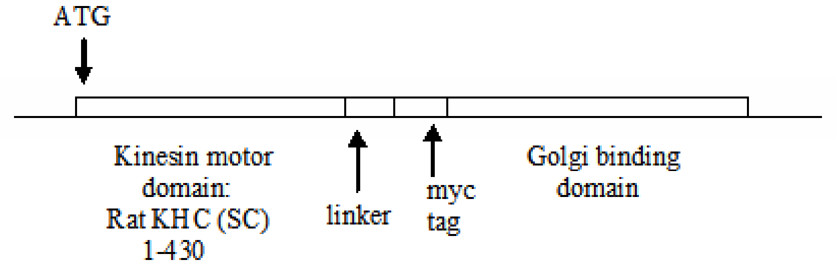

Figure 5: This is the general construct of the kinesin/Golgi fusion with the Golgi binding domains differing between fusions.

Blunt end ligation of GRIP26 and GRIP38:

After several unsuccessful attempts to clone the fusions directly into a fly vector, blunt end ligation with the Zero Blunt® TOPO® PCR Cloning Kit from Invitrogen was used for cloning. To obtain DNA for this protocol, the fusion DNA sent to us was amplified in a PCR reaction using the primer CTCACTGGCCGGCCCAAAACATGGCGGACCCAGCCGAATGC containing an FseI cut site at the beginning of the fusion sequence and ATTCTGGCTAGCCTCCCGGGGATCTCTAGA containing an NheI cut site at the end of the sequence. The reaction was set up with 10x Pfx Amplification Buffer, 10 mM dNTP mixture, 50 mM $MgSO_4$, Platinum® Pfx DNA polymerase, and primers designed to cut out the kinesin/Golgi fusion construct. The PCR reaction was run in a BioRad MyCycler thermal cycler using three cycles: Cycle 1 was only run one time at 94ºC for two minutes to denature the template DNA, Cycle 2 was repeated 35 times and consisted of a denaturing phase at 94ºC for 15 seconds, an annealing phase at 55ºC for 30 seconds, and an extending phase at 68ºC for 2 minutes, and Cycle 3 was run one time with a phase at 68ºC for 10 minutes and then a storage phase at 4ºC until the sample was removed. The PCR product was then gel purified by running the sample in a 1% agarose gel, staining with ethidium bromide, and cutting out the sample band under UV light. This PCR product was purified using the protocol of the QIAquick Gel Extraction Kit from Qiagen, which uses QIAquick columns to isolate the DNA while washing out other compounds that can pass through the column membrane with buffers. The DNA in the columns was eluted with sterile ddH_2O to use for the blunt end ligation. The protocol for the Zero Blunt® TOPO® PCR Cloning Kit ligation reaction called for reactions containing 4 µl PCR product with 1 µl dilute salt solution (300 mM NaCl and 15 mM $MgCl_2$) and 1 µl of a solution containing the TOPO® vector (pCR4-BLUNT) and an enzyme. After this reaction was incubated at room temperature for 5 minutes, it was electroporated into electrocompetent cells. The electroporation protocol used was "Electroporation of DH10B cells" from the Rose Lab Procedures Manual (Yale University). The electroporation reaction consisted of 2 µl of ligation reaction with 50 µl of DH5α electrocompetent cells and 17 µl of 10% glycerol to reduce the salt concentration of the cells. Gene Pulser® cuvettes with 0.2 cm electrode caps were used in a Biorad MicroPulser.

The preset program used on the electroporation instrument was 1 pulse at 2.5 kV with no time constant. The cells were allowed to recover after electroporation at 37ºC in S.O.C. medium (bacto-tryptone, bacto-yeast extract, NaCl, KCl, Mg^{2+}, glucose, dH_2O) while shaking at 220 RPM for one hour. They were then plated on selective ampicillin LB-Agar plates. Any colonies that grew on these plates were supposed to contain the TOPO® vector with the GRIP fusion ligated into it. Four colonies were harvested from the GRIP26 vector ligation, and six colonies were harvested from the GRIP38 vector ligation. These colonies were grown in cell culture tubes containing LB solution with ampicillin overnight until the cultures were saturated. Glycerol stocks were made from this DNA and frozen at -80ºC for future use. A Mini-Prep was performed with this DNA using the Promega Wizard Plasmid DNA Mini-Prep kit and following the Promega Wizard protocol steps 1-10 and then Michael Freitag's "Alkaline Lysis of Overnight E. coli cultures" protocol. This alternative protocol washes the DNA pellet obtained using isopropanol and 70% ethanol before resuspending in TE buffer. The Mini-Prep DNA obtained was digested with the enzymes XbaI and FseI in a reaction containing New England Biolab (NEB) restriction digest buffer 4 and BSA. These digests were analyzed in 0.8% agarose gels for a band the size of the kinesin/Golgi fusion (1726 bp for GRIP26 and 1451 bp for GRIP38) and a band the size of the pCR4-BLUNT vector, which was about 4000 bp. For GRIP26, one digest showed the right cutting pattern, meaning that one electroporated cell contained correctly ligated plasmid. For GRIP 38, three cells seemed to have picked up the vector containing the fusion. For both GRIP vectors, one glycerol stock of bacteria containing the ligated fusion and vector was used to start overnight saturation cultures for Midi-Preps. The Midi-Preps were performed using the QIAGEN Plasmid Midi Kit. The DNA obtained from the

Midi-Preps was resuspended in TE buffer and quantified using a BioRad SmartSpec™ Plus spectrophotometer. This DNA was diluted to 0.5µg/µL to store.

Cloning of GRIP26 and GRIP38 into pUAST::3YCT vector:

Part of this DNA was used in a restriction enzyme digest of both the pCR4-BLUNT::GRIP vectors and the pUAST::3YCT vector into which the fusion was ultimately being inserted. The restriction digests were set up with NEB Restriction Digest Buffer 4, BSA, the restriction enzymes XbaI and FseI, and the appropriate DNA. The FseI site was at the beginning of the fusion sequence and the XbaI site was at the end. The digest cut out the three YFP sequences in the pUAST::3YCT vector. These digests were incubated overnight and then run in a 1% agarose gel. The DNA was cut out of the gel and purified using the QIAGEN QIAquick Gel Extraction Kit. To ligate the GRIP26 DNA into the pUAST::3YCT vector, two ratios of vector to insert were used: 1 µl of vector to 3 µl of insert and 2 µl of vector to 4 µl of insert. Since the 2:4 ratio of vector to insert was more efficient, that was the ratio used for the later GRIP38 ligation. The DNA mixtures were initially heated at 65ºC for 5 minutes to free any sticky ends that had associated with one another using a program on the BioRad MyCycler thermal cycler. T4 DNA ligase and T4 DNA ligase buffer were then added to the DNA mixture and the thermal cycler program incubated the reaction at 16ºC overnight. It was reheated to 65ºC for 10 minutes the following morning to make sure that all DNA had properly annealed and to separate any DNA that had not. The ligation reaction was electroporated into a 75% solution of DH5α cells diluted with 10% glycerol to lower their salt concentration to prevent arcing. The electroporation was performed by following the "Electroporation of DH10B cells" protocol from the Rose Lab Procedures Manual. The electroporation procedure used the same settings listed previously and the cells recovered in S.O.C. medium while shaking at 200 RPM for 1 hour. The cells were plated on selective ampicillin (1.5 μg/mL) LB-Agar plates and incubated at 37ºC. Ten colonies were picked from the GRIP26 plates and eight colonies from the GRIP38 plates to use for making overnight saturation cultures in LB media containing ampicillin. The cultures were then used to make glycerol stocks and to do Mini-Preps of the DNA with the Promega Wizard Plasmid DNA Mini-Prep kit as previously described. The Mini-Prep DNA was resuspended in TE buffer. As a diagnostic tool to analyze whether any of the cells had picked up the correctly ligated vector and fusion, some of the DNA was digested with XhoI in a reaction containing NEB restriction digest buffer 2 and BSA. XhoI cut both the insert and vector and was expected to cut out a 268 bp band in both the GRIP26 and GRIP38 vectors. The digests were incubated overnight at 37ºC and then were run in a 1% agarose gel to check if they were cut as expected. Nine of the ten GRIP26 preps seemed to contain the correct DNA showing a band at 268 bp. All eight of the GRIP38 preps showed the band at 268 bp, but three of the samples also showed an unexpected third band, so those preps were not used further. One DNA prep was chosen for both GRIP26 and GRIP38 and the glycerol stocks were used to grow up DNA for Midi-Preps. The Midi-Preps were performed as before using the QIAGEN Plasmid Midi Kit Protocol. Once the DNA was quantified on the BioRad SmartSpec™ Plus spectrophotometer, it was diluted to a concentration of 0.5 μg/μl for storage.

Cloning GRIP22:

GRIP22 was cloned by Greg Kothe without using the blunt end vector intermediate step. Instead, he cut the fusion out of the original vector using SpeI and XbaI. Because GRIP22 contains an internal XbaI cut site, digesting with these enzymes cut the insert into two pieces which were then ligated into the pUAST vector to form pUAST::GRIP22. After electroporation and selective plating, 20 colonies were picked with which to perform Mini-Preps. These preps were analyzed by restriction digest with SpeI and XbaI to look for 3 bands of sizes 362 bp, 1.7 kb, and 9-10 kb. From this analysis, 17 of the preps seemed to have the right DNA. The DNA for these Mini-Preps was then given to me by Dr. Kothe so that I could continue by sequencing and eventually injecting this fusion.

Sequencing DNA:

DNA that seemed to contain the correctly ligated GRIP insert and vector could be delivered to the Nucleic Acid Facility at Penn State for sequencing. In order to do this, some of the Mini-Prep DNA was precipitated with ethanol, resuspended in ddH_2O, and diluted to a solution of 0.3 µg/µl. Two sequencing primers were designed within the shared fusion sequences that could be used for all three fusions, a third primer in the SV40 region of the vector just outside of the fusions, and a fourth primer in the hsp70 vector sequence (GACAAAATAAGGGACTTGCTTGACG, CTTGGAACTAACAGCAGAAGAATGG, CTTTAAATCTCTGTAGGTAGTTTGTCC, and AGCGCAGCTGAACAAGCTAAAC, respectively). After seeing several consistent mutations appear in sequencing results of several GRIP22 clones, I thought that the original GRIP sequences sent to me might have mutations. Thus, I designed a primer (GAACCCACTGCTTAACTGGC) just outside of the fusion sequence in the GRIP22 source vector sent to me by Sean Munro and prepared some of this DNA for sequencing. When those sequence results came back, I found that there were two mutations in the fusion DNA: a G to C change at 104 nt of the expected DNA sequence and an A to C change at 573 nt of the expected sequence. The G to C change would change that codon to code for alanine instead of glycine. Since both alanine and glycine are nonpolar amino acids, this change may not alter the function of the protein. The A to C change would be silent because both codons would code for arginine. I assumed that the constructs had these mutations when they were used by Dr. Munro since all three of the fusions contained the mutations. If so, the mutations did not inhibit the function of the proteins when he used them. Clones for each of the GRIP fusions were found that had no further mutations and these clones were chosen for injection into flies.

Injecting into flies:

Midi-Prep DNA for each of the GRIP fusions was combined with the helper plasmid Δ2-3 for injection. This DNA combination was precipitated and then suspended in injection buffer dyed with food coloring for easy visualization during injection. *Drosophila* embryos from a yw fly line were collected on "apple caps" (made from apple juice concentrate, dH_2O, sucrose, agar, and propionic acid) with a dab of yeast paste for the flies to eat. The embryos were injected within two hours of collection (collected for one hour and injected for one hour) by lining embryos up on a coverslip and injecting into the posterior ends. An inverted microscope with a micromanipulator to adjust the needle was used for injection. The needle was attached to an air-pressure injecting device for propelling DNA out of the needle into the embryos. DNA was spun down for 15 minutes before injecting so that any solids in the prep would not clog up the needle and was then loaded into the needle using a syringe.

Genetics of injected flies:

Injected embryos were placed in food vials to develop into adult flies. Both males and females were mated with Gla/CyO lines. Orange-eyed males were collected from these crosses and mated with yw females. From these crosses, progeny were used to identify the fly chromosome in which the GRIP fusion was inserted. Since the injected flies (yw) were originally mated to a Gla/CyO line, where Gla and CyO are on the second chromosome, all orange-eyed flies contained either Gla or CyO. These markers could then be used to map the GRIP transgene to a certain chromosome.

If the progeny of the cross of orange-eyed males to yw had no orange-eyed flies with Gla or CyO, this meant that the transgene had inserted in the second chromosome. If there was a mixture of the markers and wild type (yw) with the orange-eyed and white-eyed flies, this meant that the transgene was in the third chromosome. Finally, if there were no orange-eyed males and all females were orange-eyed, both sexes containing a mixture of Gla or CyO and wild type, this meant that the transgene was in the X chromosome. Once these lines were mapped, they were balanced by crossing them to a baz^4/FM7c line for the X chromosome, a Gla/CyO line for the second chromosome, and a G1/TM6B line for the third chromosome. This is outlined in Figure 6. Where possible, two lines of each GRIP transgene were kept for all chromosomes. The names for all transgenic insertions for each fusion are listed in Table 1.

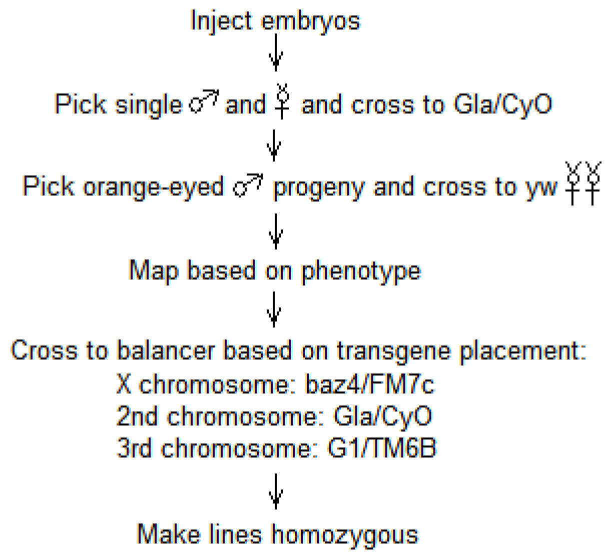
Inject embryos
Pick single ♂ and ♀ and cross to Gla/CyO
Pick orange-eyed ♂ progeny and cross to yw ♀♀
Map based on phenotype
Cross to balancer based on transgene placement:
X chromosome: baz4/FM7c
2nd chromosome: Gla/CyO
3rd chromosome: G1/TM6B
Make lines homozygous

Figure 6: Genetic scheme for transgenic fly lines.

Table 1: This table contains the names of the lines that inserted on each chromosome for the three fusions. They were based on the letter or number assigned to crosses made after injection.

Transgenic line names			
Fusion	Chromosome X	2nd chromosome	3rd chromosome
GRIP22	I.1, I.2	V.7, V.8	V.2, V.3
GRIP26	none	JJ.1, JJ.3	JJ.2, JJ.5
GRIP38	2.5	1.1, 2.6	3.10, 4.5

Once the lines were balanced and heterozygous, homozygous flies were crossed to make homozygous lines without balancers. These flies could then be used to observe any phenotypes due to removing the Golgi.

Antibody staining:

In order to look at Golgi a different way and see if the fusions were being expressed, larvae were dissected into filets and stained with antibodies to a Golgi protein or the myc linker. For the Golgi staining, a UAS-mCD8-RFP × UAS-GalT-YFP cross was used. For the myc staining, the GRIP fusions were evaluated with a 477-Gal4;UAS-GalT-YFP × UAS-mCD8-mRFP;GRIP cross with GRIP26 JJ.2, GRIP26 JJ.5, GRIP22 V.2, and GRIP38 3.10. A 477-Gal4,UAS-mCD8-RFP × UAS-tau-myc-GFP cross was used as a positive control.

To do the dissections, wandering third instar larvae were used because it was easier to work with larger larvae. The larvae were dissected on a dissecting dish, a small petri dish containing a layer of agar gel in which to insert pins in the larvae. The larvae were pinned at the head and tail with dorsal side facing up and then cut with micro-dissecting scissors between the tracheae along the length of the larvae while covered in Schneider's media. The guts of the larvae were gently removed with forceps, leaving the brain when possible. The empty cuticle was spread and pinned with six pins on the sides (Figure 7). Once a larva was dissected, a drop of 4% paraformaldehyde (PF) was used to fix its shape. After soaking in PF solution while other larvae were dissected, the pins were removed and the larvae were placed in 4% PF in a microcentrifuge

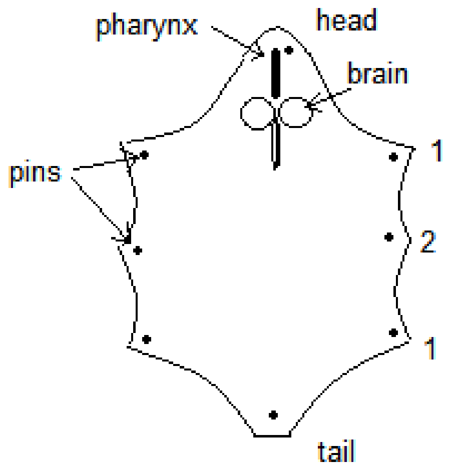

Figure 7: Drawing of fully stretched out and pinned larval filet

tube. The larval filets were washed in block solution (0.2% TX-100, 10 mM glycine, 1% BSA in PBS) five times for 10 minutes per wash while gyrating on a rocker. The primary antibody was then added to the larvae. For imaging the Golgi, the primary antibody was rabbit α-GM130 and a 1:400 ratio of antibody to block was used for staining. To evaluate expression of the kinesin/Golgi fusion, the primary antibody used was mouse α-c-myc in a 1:100 ratio to block solution. The larval filets were allowed to incubate in antibody overnight while rocking in the cold room at 4ºC. The next day, the antibody/block solution was removed and the larvae were washed six times for 20 minutes each time in fresh block solution. After washing, the secondary antibody was added in a ratio of 1:400 antibody to block. For the GM130 antibody, a Cy5 goat α-rabbit secondary antibody was used and for the myc antibody, a Cy5 mouse α-rabbit secondary antibody was used. The secondary antibody was incubated with the larval filets for one hour at room temperature while gyrating. The secondary antibody was then removed and the filets were washed four times for 15 minutes each with fresh block. The final wash was replaced with 85% glycerol/50mM Tris pH8. The microcentrifuge tubes containing the filets were wrapped in foil and stored at 4ºC overnight in the refrigerator until ready to be imaged. To image the filets, one was placed on a glass slide in a little of the glycerol/Tris solution in which they were stored and a coverslip was taped down over them.

GRIP lines:

The Golgi marker UAS-GRASP65-GFP was used with both the lva RNAi and the GRIP fusions. Thus, it was combined with UAS-dicer2 and elav-Gal4 as the driver into the line UAS-GRASP65-GFP;elav-Gal4,UAS-dicer2. The genetic scheme for making this line is shown in Figure 8.

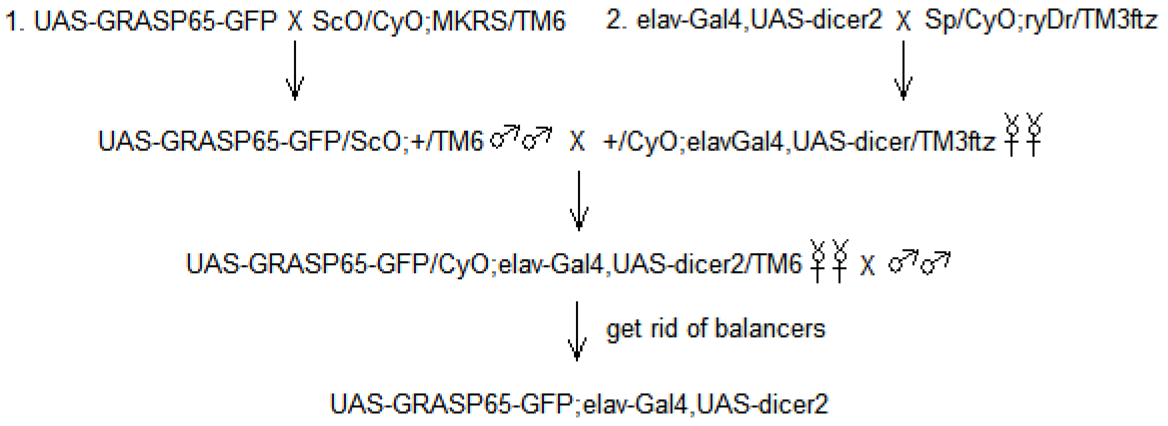
1. UAS-GRASP65-GFP X ScO/CyO;MKRS/TM6
2. elav-Gal4,UAS-dicer2 X Sp/CyO;ryDr/TM3ftz
UAS-GRASP65-GFP/ScO;+/TM6 ♂♂ X +/CyO;elavGal4,UAS-dicer/TM3ftz ♀♀
UAS-GRASP65-GFP/CyO;elav-Gal4,UAS-dicer2/TM6 ♀♀ X ♂♂
get rid of balancers
UAS-GRASP65-GFP;elav-Gal4,UAS-dicer2

Figure 8: Genetic scheme for making GRASP65-GFP;elav-Gal4,UAS-dicer2 line.

Later lines were made with the Golgi markers UAS-ManII-EGFP and UAS-GalT-YFP. Since ManII-EGFP is on chromosome 2, a recombinant was made with the driver 109(2)80: 109(2)80,UAS-ManII-EGFP (Figure 9).

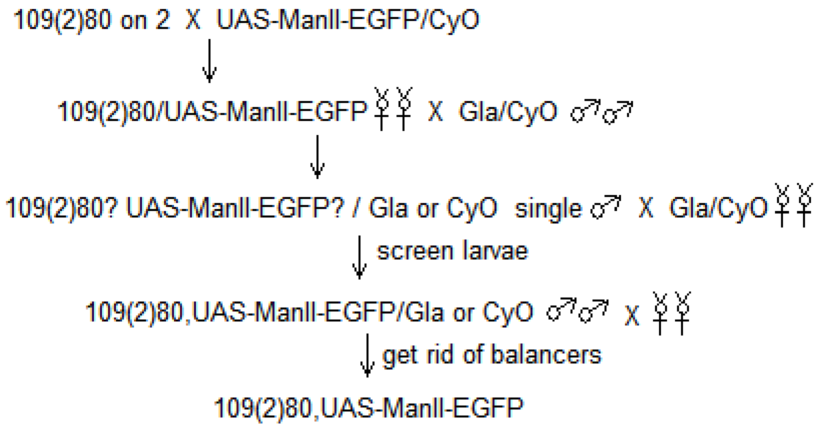
109(2)80 on 2 X UAS-ManII-EGFP/CyO
109(2)80/UAS-ManII-EGFP ♀♀ X Gla/CyO ♂♂
109(2)80? UAS-ManII-EGFP? / Gla or CyO single ♂ X Gla/CyO ♀♀
screen larvae
109(2)80,UAS-ManII-EGFP/Gla or CyO ♂♂ X ♀♀
get rid of balancers
109(2)80,UAS-ManII-EGFP

Figure 9: Genetic scheme for making 109(2)80,UAS-ManII-EGFP line.

The GalT marker was on chromosome 3, so it was recombined with the driver 221Gal4 that expresses in class I da neurons to make the line 221Gal4,UAS-Gal4-YFP (Figure 10). For imaging, these were to be crossed to a line made with the membrane marker mCD8-RFP and the GRIP fusion lines that had inserted on chromosome 3 (Figure 11). These lines were then crossed so that the Golgi could be visualized with mCD8-RFP outlining the neurons and their processes.

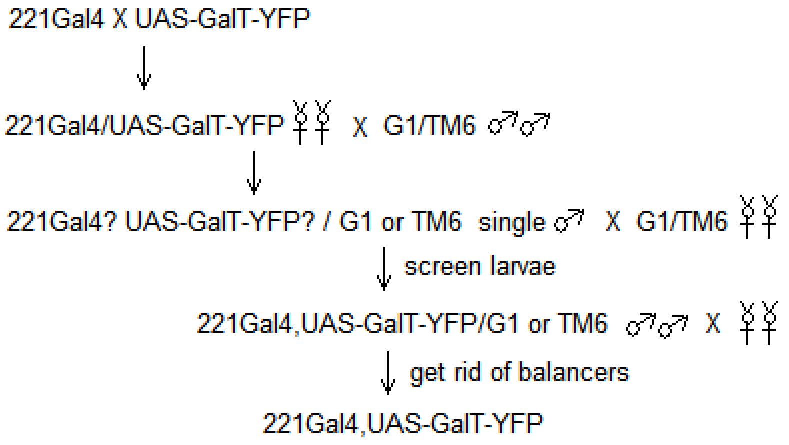
221Gal4 X UAS-GalT-YFP
221Gal4/UAS-GalT-YFP ♀♀ X G1/TM6 ♂♂
221Gal4? UAS-GalT-YFP? / G1 or TM6 single ♂ X G1/TM6 ♀♀
screen larvae
221Gal4,UAS-GalT-YFP/G1 or TM6 ♂♂ X ♀♀
get rid of balancers
221Gal4,UAS-GalT-YFP

Figure 10: Genetic scheme for creating 221Gal4,UAS-GalT-YFP line.

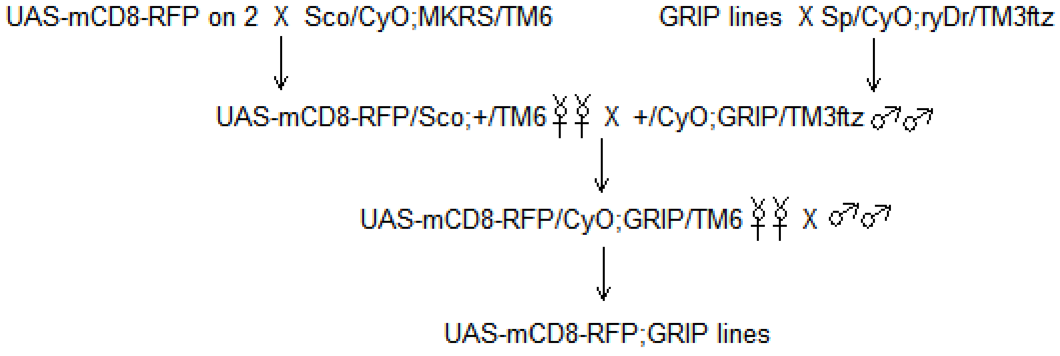
UAS-mCD8-RFP on 2 X Sco/CyO;MKRS/TM6
GRIP lines X Sp/CyO;ryDr/TM3ftz
UAS-mCD8-RFP/Sco;+/TM6 ♀♀ X +/CyO;GRIP/TM3ftz ♂♂
UAS-mCD8-RFP/CyO;GRIP/TM6 ♀♀ X ♂♂
UAS-mCD8-RFP;GRIP lines

Figure 11: Genetic scheme for making UAS-mCD8-RFP;GRIP fusion lines.

Fly lines:

Since I had decided to focus on the GalT-YFP Golgi marker, I used the driver 477-Gal4, which expresses in class IV neurons, to make a 477-Gal4;UAS-GalT-YFP line by the genetic scheme shown in Figure 12. For imaging, this line was crossed to the UAS-mCD8-RFP;GRIP lines previously described to visualize the Golgi in class IV neurons of the transgenic GRIP fusion lines. As a control, the 477-Gal4;UAS-GalT-YFP line was crossed to UAS-mCD8-RFP alone.

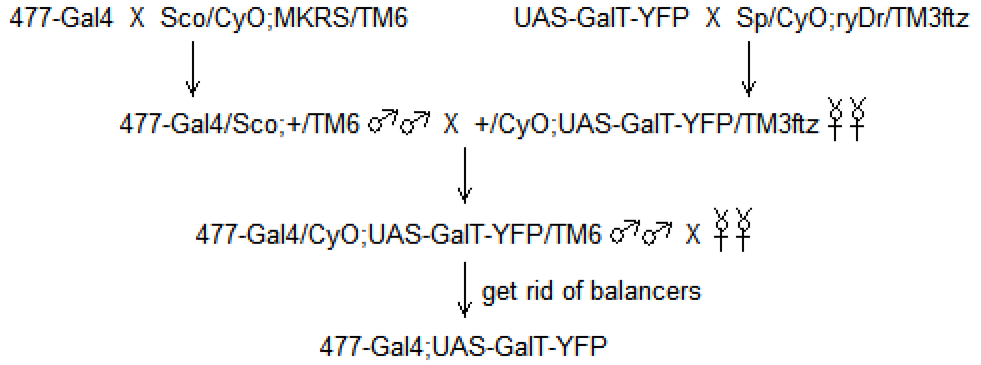
477-Gal4 X Sco/CyO;MKRS/TM6
UAS-GalT-YFP X Sp/CyO;ryDr/TM3ftz
477-Gal4/Sco;+/TM6 ♂♂ X +/CyO;UAS-GalT-YFP/TM3ftz ♀♀
477-Gal4/CyO;UAS-GalT-YFP/TM6 ♂♂ X ♀♀
get rid of balancers
477-Gal4;UAS-GalT-YFP

Figure 12: Genetic scheme for making 477-Gal4;UAS-GalT-YFP

Lva RNAi:

To use another technique to image the effect of Golgi depletion, lines were set up containing lva RNAi along with the protein dicer2 for better RNAi knockdown. Using the driver 109(2)80, which expresses in all da neurons, the line UAS-EB1-GFP,109(2)80;UAS-dicer2 was made and crossed to a lva RNAi line provided by VDRC (VDRC#40382, CG6450). As a control for this experiment, I used the same line crossed to ncd RNAi. From these crosses, embryos were collected daily so that larva would be approximately the same age (within 24 hours) and larva were imaged four days after the embryos were collected when they were in the 3rd instar stage. The embryos were collected on apple caps (made of apple juice concentrate, dH$_2$O, sucrose, agar, and propionic acid) and then transferred to food vials to grow into larvae. Some of the larvae were kept from moving by incubating them in a mixture of 1 part chloroform to 4 parts halocarbon oil for 2 minutes. Then they were placed onto a slide in a drop of the chloroform/oil mixture and a coverslip was taped on top of them. Later on in the experiment, slides containing a dried drop of 3% agarose were used to pull moisture out of the larval cuticle and hold the larvae in place. A coverslip was taped on top of these agarose slides.

Microscopy:

To image larvae from the lines made, either an LSM 510 Zeiss Confocal microscope or an Olympus FluoView 1000 Confocal microscope was used. The lva and ncd RNAi larvae were all imaged on the Zeiss microscope under a 488 nm laser to show GFP expression with a 63x objective lens. The majority of the rest of the images were taken on the Olympus microscope with a 488 nm laser to show GFP expression and a 546 nm laser to show RFP expression. These images were taken with 60x or 40x objectives. When the Cy5 protein was used for antibody staining, it was imaged on the Olympus using a 635 nm laser.

CHAPTER 1: ARE THE FUSIONS BEING EXPRESSED?

In order to evaluate whether the Golgi were nucleating microtubules in *Drosophila* dendrites, I wanted to move the Golgi out of dendrites using kinesin/Golgi fusion proteins. Kinesin is a motor protein that walks along microtubules. It binds to cargo such as organelles and vesicles and transports these throughout the cell. The classic kinesin structure is a protein dimer that intertwines to form the kinesin. It consists of a heavy chain that composes the motor domain of the protein. The light chain forms the tail region where the cargo binds. These two domains are connected by a flexible coiled-coil region that can change conformation and move the kinesin along the microtubule. This movement is caused by ATP hydrolysis and release of ADP. Motor proteins walk along microtubules in only one direction because they can only bind to the microtubule in one orientation. Many kinesins walk towards the plus ends of microtubules, but some kinesins and another class of motor proteins, dyneins, walk towards the minus ends. The kinesin that used in the fusions walks towards the plus end of microtubules. In these fusion proteins, the kinesin will be bound to Golgi and should pull Golgi outposts towards microtubule plus ends. This should move Golgi outposts from the dendrites in towards the soma and possibly out into the axons.

Once the fusions had been cloned into flies, I wanted to see if they were actually being expressed. Since I was using vectors that contained mammalian proteins, I did not know whether or not the proteins made in flies would be stable and functional. To address whether the mammalian proteins might function in flies, I performed BLAST homology searches comparing the protein sequences of the kinesin and Golgi domains being used from mammals with the *Drosophila* genome. According to the BLAST search with the rat KHC domain, 61% of the amino acids were identical and the E value, the expected times that one would see this overlap by chance, was 0.0 (too small to be expressed by the program). Thus, there is significant homology in the KHC domain and it can be expected to work in *Drosophila*. For the human GMAP210 protein used in GRIP22, the BLAST search showed 28% amino acids as identical and had an E value of $6e^{-20}$. Thus, there is homology between *Drosophila* and the human sequence, but it is not as similar as the KHC domain. The BLAST search for the human golgin-97 protein in GRIP26 showed 26% identical amino acids and an E value of $5e^{-28}$, which is similar homology to the GMAP210 protein and is again less similar than the KHC domain. In addition to this information, these fusions were used previously in a *Drosophila* cell line where they worked to move the Golgi (Sean Munro, personal communication).

In order to evaluate the expression of the fusions in my fly lines, I stained with an antibody against the protein c-myc, which was used as a tag in the linker of the GRIP constructs (Figure 5). This antibody staining was done in larval filets dissected such that only the cuticle and brain of the larvae were left intact and the guts were removed. This allowed me to easily stain and then visualize the da neurons just inside the cuticle. Through this process, I was able to see how much myc was being expressed in the larvae, which was a good indication of how much the fusions were expressing.

RESULTS

I stained my dissected larval filets with a c-myc antibody to look for expression of the GRIP fusions in various lines. A UAS-tau-myc-GFP line served as a positive control to show whether the myc antibody worked and what myc would look like in a neuron stained with the antibody (Figure 13). The same primary antibody/block mixture was used for all of the myc staining except for several of the early GRIP26 JJ.2 dissections, which were done with a 1:400 mixture of antibody to block that I later decided might not be concentrated enough to show much myc (data not included in Table 2). Thus, I assumed that the myc staining pattern in the tau-myc-GFP line was probably similar to the myc staining pattern I would see in the GRIP lines if the fusions were being expressed. The expression of myc in the tau-myc-GFP line was quite high (635nm laser power was generally at or below 1%) and there seemed to be expression throughout the soma, dendrites, and axon of each neuron. The myc staining in the 477-Gal4;UAS-GalT-YFP × UAS-mCD8-mRFP;GRIP38 3.10 cross seemed to be fairly similar to the tau-myc-GFP staining pattern, although the myc staining was not so bright in the GRIP38 neurons (Figure 13). Also, only about half of the GRIP38 neurons showed myc staining at a significant level, which I considered to be at or below 20% laser power of the 635nm (Cy5) laser (Table 2). The GRIP38 expression pattern contrasts greatly with GRIP26 JJ.2 expression in the 477-Gal4;UAS-GalT-YFP × UAS-mCD8-mRFP;GRIP26 JJ.2 cross. All of these GRIP26 JJ.2 neurons showed very low levels of myc staining and the 635nm laser had to be turned up to 40% in order to see a complete outline of the soma (Figure 13 and Table 2). When I could see myc expression in these neurons, it seemed to be mostly in the soma and not in axons or dendrites. I considered myc expression only visible at 40% laser power likely to be bleedthrough from the other fluorescent proteins (GFP or RFP) rather than true Cy5 signal. When I looked at the 477-Gal4;UAS-GalT-YFP × UAS-mCD8-mRFP;GRIP26 JJ.5 cross, there seemed to be higher expression of the fusions. Five larvae were dissected and 15 of the 18 neurons evaluated showed medium to high myc expression (Table 2). The majority of these neurons had medium expression of myc, which suggests a lower expression of the fusions than in the GRIP38 3.10 line, but a greater proportion of these neurons expressed some myc than the GRIP38 3.10 neurons. There is clearly more expression in the GRIP26 JJ.5 line than in the GRIP26 JJ.2 line. In looking at the 477-Gal4;UAS-GalT-YFP × UAS-mCD8-mRFP;GRIP22 V.2 cross, I saw fairly consistent myc expression around 20% laser power (Table 2). This line was not as variable in its myc expression, but did not express as highly as some of the GRIP38 3.10 or GRIP26 JJ.5 neurons. Also, all of the neurons seemed to be expressing myc somewhat. However, this line has very low levels of mCD8-RFP expression, so it was not used for looking at Golgi in the neurons.

Table 2: This table shows the myc expression data in some of the GRIP fusions according to "low," "medium," and "high" expression levels set based on the distinctions seen in the images. The GRIP38 fusion is the control that does not contain a Golgi domain. The GRIP26 fusion contains the C terminus of the trans Golgi protein golgin-97 as its Golgi domain. The GRIP22 fusion contains the C terminus of the cis Golgi protein GMAP210 as its Golgi domain.

GRIP fusion larval filet myc expression			
Fusion (n=number of neurons)	Low expression (40% laser power)	Medium expression (11-20% laser power)	High expression (10% laser power and below)
GRIP38 3.10 (n=19)	9	2	8
GRIP26 JJ.2 (n=20)	20	0	0
GRIP26 JJ.5 (n=18)	3	10	5
GRIP22 V.2 (n=14)	0	13	1

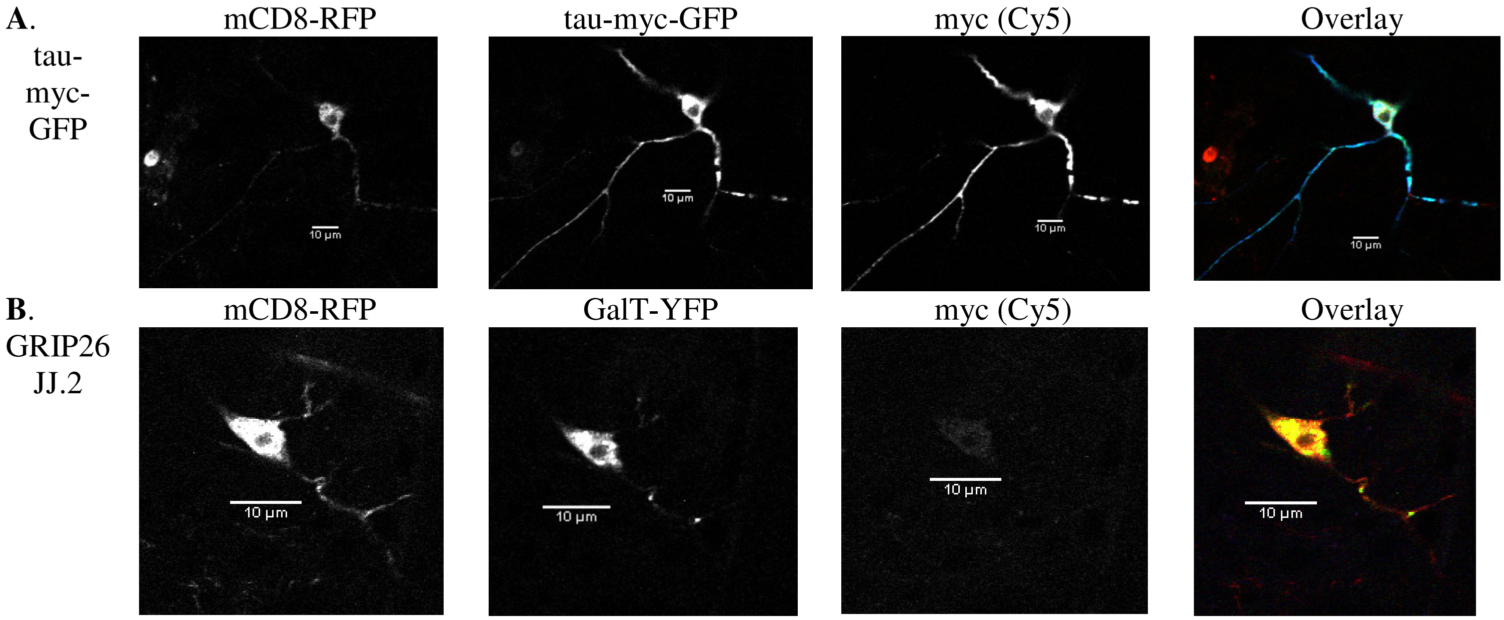

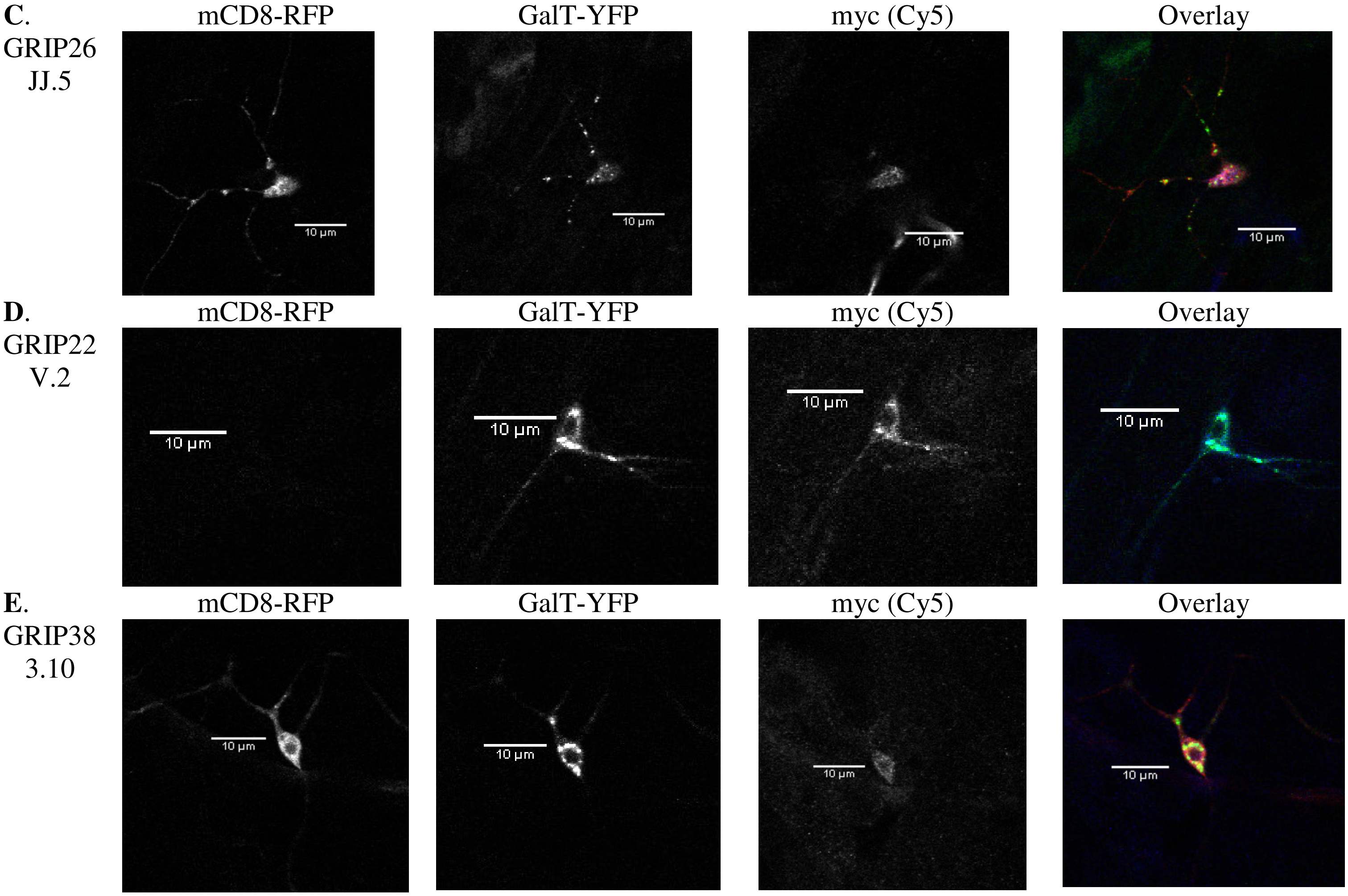
C.
GRIP26
JJ.5
mCD8-RFP
GalT-YFP
myc (Cy5)
Overlay
10 µm
D.
GRIP22
V.2
mCD8-RFP
GalT-YFP
myc (Cy5)
Overlay
10 µm
E.
GRIP38
3.10
mCD8-RFP
GalT-YFP
myc (Cy5)
Overlay
10 µm

Figure 13: Results of antibody staining with α-c-myc as the primary antibody and Cy5 attached to the secondary antibody.

A. This is a sample image of the tau-myc-GFP control line that was crossed to 477-Gal4 so that it would express only in the class IV neuron. The stained myc was expressing at quite a high level (laser at 0.5%), which is apparent since blue is the most prominent color in the overlay. The red color in the overlay image represents mCD8-RFP, the green represents tau-myc-GFP, and the blue represents Cy5 expression of myc.

For the overlay images in B-E, mCD8-RFP is represented in red, GalT-YFP is represented in green, and myc is represented in blue. The single channels are shown in grayscale for higher clarity.

B. This is one of the GRIP26 JJ.2 neurons that showed very little Cy5 fluorescence from myc staining (laser at 40%), which is why barely anything is visible in the myc image.

C. This is one of the GRIP26 JJ.5 images showing high Cy5 fluorescence from myc staining, mostly in the cell body (laser at 7%).

D. This is one of the GRIP22 V.2 images showing medium Cy5 fluorescence from myc staining (laser at 20%) and no visible mCD8 expression.

E. This is one of the GRIP38 3.10 neurons in which I saw fairly little Cy5 fluorescence from myc staining (laser at 40%).

Discussion

The main idea behind antibody staining was to evaluate whether or not the GRIP fusions were being expressed in cells. Because there was a myc tag in between the kinesin and Golgi domains in each of the GRIP fusions (Figure 5), I used an antibody to myc to see where myc was being expressed. If there was myc expression, this would show that the GRIP fusion was being expressed in the cell. In order to evaluate whether or not the c-myc antibody worked well and if my staining procedure would show myc, I looked at a tau-myc-GFP line. Staining this line showed me very high expression levels of myc throughout the neuron, meaning that the antibody did work to stain myc. I expected to see tau most intensely in the proximal axons, some in the cell bodies, and possibly a little in the dendrites (Rolls et al., 2007). Thus, I wonder if the antibody mixture could have been too concentrated and it stuck to the whole neuron more than it should have. However, I basically saw the pattern that I would have expected, so I did know that the antibody should work and I should see it in the GRIP fusions if they were being expressed.

When I first started dissecting the GRIP fusions, I was still practicing my dissection skills and the neurons in the filets were often mangled and the staining was not consistent. Thus, I was concerned that I would not be able to truly tell what the expression patterns were. However, I did see clear differences in the expression levels in the various GRIP lines. In the GRIP26 JJ.2 line, there was very little if any myc expression at all. The laser had to be up quite high to see any Cy5, which makes me think that the fluorescence I was seeing was mostly bleedthrough from the RFP or GFP. If I did see some expression, it mostly seemed to be in the soma and not out in the axons or dendrites. The expression also was not clearly colocalized with the Golgi revealed by the GalT-YFP marker.

The other GRIP lines all showed more myc expression than GRIP26 JJ.2. The GRIP26 JJ.5 line showed the majority of neurons (10 out of 18) having a medium expression of myc where the laser power was between 11 and 20%. I would consider this to be a level that is not due to simply bleedthrough of the other fluorescent proteins and shows actual expression of myc, even though it is much less than that seen in the tau-myc-GFP line. The difference in expression level between the tau-myc-GFP line and the fusions could be due to the fusion products not being very stable in the cell when they are made. They could also be in a region of the genome where they are transcribed less and are therefore less prevalent in the cell. The expression in these neurons was very inconsistent, which makes it hard to draw conclusions about the expression of the fusions in this line. The three neurons that showed low Cy5 expression were all from the same larval filet, suggesting that this larva either did not stain properly or was not expressing the fusions. It is certainly possible that the staining was inconsistent since I did often see variation between filets of the same line that were stained together. According to others in the Rolls lab with experience dissecting and staining, the antibody penetration of the filets can be variable. Thus, much of the variation I saw between filets could have been due to variation in the staining. The other explanation would be that the variation is within the GRIP lines. Since the lines containing the fusions being used were UAS-mCD8-mRFP;GRIP and contained both the fusion and mCD8-RFP, one would expect that if the fusion were not being expressed, mCD8 would not be expressed either. This could be a problem if balancers were not completely removed from the line and some of the flies were thus heterozygous for UAS-mCD8-mRFP;GRIP rather than homozygous. However, the lines made for GRIP26 JJ.5, GRIP22 V.2, and GRIP22 V.3 showed variable levels of mCD8 expression, which seemed to be unrelated to the fusions but a problem in the mCD8-RFP itself since this inconsistency also showed up in other lines that were made. Thus, mCD8 is not a good indicator of whether or not the fusion is being expressed. Sometimes there would be lots of RFP signal, sometimes there would be very little, and sometimes there would be none visible at all. However, it is hard to know whether these lines actually were not expressing both mCD8-RFP and the fusions, or whether only the RFP was not being expressed. In the GRIP26 JJ.5 dissected lines, the three neurons expressing low levels of Cy5 were all from a larva not expressing RFP. Thus, it seems likely that this larva was not expressing either mCD8-RFP or the fusion. However, there was another GRIP26 JJ.5 larval filet that was not expressing RFP but the five neurons imaged from this larva were showing moderate levels of Cy5 with the 635nm laser power at 20%. I would say that this neuron seemed to be expressing the fusions since there was some myc expression. This would mean that this larva was expressing the fusion but not mCD8-RFP because of the inconsistency of the line. However, it could also be possible that this moderate myc expression is showing up because the antibody is binding to something besides the fusions and showing low levels of expression. I cannot know what is really happening, but I am going to assume that the moderate expression of Cy5 with the laser power up to 20% is showing a low level of the fusion being expressed in the cell and that if I see that amount of expression, the fusion is being expressed whether or not there is mCD8-RFP expression. Based on this, four out of five of the GRIP26 JJ.5 larvae dissected seemed to be expressing the fusions at some level, which varied but was never as bright as the tau-myc-GFP control.

In the staining of the GRIP22 V.2 lines, I saw much more consistent levels of Cy5 expression. Thirteen out of fourteen neurons (from five larval filets) showed moderate levels of myc expression and one of them showed higher expression. This suggests a fairly consistent, low level of expression of the fusions in this line. However, none of the larvae that I dissected were expressing much mCD8 and there was generally very low mCD8 expression in this line, which meant that I could not see an outline of the neurons to be able to look at the position of the Golgi. But it also meant that once again, these neurons might not be expressing the fusions at all. In two of the five larval filets, I could see a little bit of RFP signal, which makes me think that the mCD8 is probably just expressing at very low levels because of variation in my original mCD8-RFP line, and that the GRIP22 fusion really is being expressed. Thus, I concluded that in this line, the fusion was probably being expressed at fairly low levels.

The myc expression seen in all of these fusion lines was always highest in the soma, although some expression could often be seen in the processes. It did not seem to localize consistently to somatic Golgi or any specific points, although there were sometimes little spots of Cy5 expression that could be seen. Sometimes one of these spots of high expression would overlap with Golgi, but they did not seem to be arranged in any recognizable pattern. The highest Cy5 expression in the soma is what I would expect if the fusion had pulled the dendritic Golgi outposts into the soma. However, the Cy5 signal never seemed to be very tightly localized to the Golgi in the soma.

The GRIP38 fusions were controls because they should be expressing myc hooked up to the kinesin domain, but not attached to a Golgi domain. Thus, it should not affect the Golgi or localize to Golgi. The Cy5 expression in about half of the neurons I looked at was fairly high and seemed to be spread throughout the soma, axons, and dendrites. However, I only saw this high level of expression in about half of the neurons. Sometimes the neurons within one larva varied from high to low expression levels of myc. This makes me think that the staining was inconsistent, which is a problem when trying to compare these neurons to those of the other fusions. However, the tau-myc-GFP controls did show more consistently high levels of expression without this variation, so the inconsistent levels of Cy5 could actually be due to varying levels of the GRIP38 fusion being expressed. The variations within one larval filet are probably due to varying penetration of the antibody. But overall it looks like I stained three larvae with generally high expression of the fusion and two larvae with low expression. In this line, I did not see as much mCD8-RFP variation and all of these neurons were expressing RFP. Thus, the low expression of myc is not linked to the mCD8-RFP;GRIP38 3.10 line not being expressed, but to a variation in the expression of the fusion product in certain larvae. Since I saw the most expression of mCD8 in the GRIP38 fusion line, which was the control that was not moving the Golgi, and the GRIP26 JJ.2 line, which seemed to not be expressing the fusion protein, it is possible that mCD8 expression is disrupted when there are fewer Golgi in the dendrites.

Even though these myc staining results were not always clear, it appears that I saw no real expression of the GRIP26 fusion in the JJ.2 line, but some level of expression of the fusions in all of the GRIP26 JJ.5, GRIP22 V.2, and GRIP38 3.10 lines. Thus, I would expect the fusions to work better and show more of a phenotype in the GRIP26 JJ.5 and GRIP22 V.2 lines than in the GRIP26 JJ.2 line.

CHAPTER 2: WHAT CAN I USE TO BEST VISUALIZE THE GOLGI?

In order to visualize Golgi in the neurons using live microscopy, I needed a good GFP marker that would localize only to Golgi and would not alter the distribution of Golgi in the neuron. If the marker localized to other organelles or membranes, I would never know if the spots of GFP were actually Golgi. And if the marker changed the cellular distribution of Golgi, I might be unable to detect the effect that the fusions lines would have on the cell and I would also think that the Golgi were normally distributed differently than they actually are. Thus, I looked at several different Golgi markers to find one that would work well.

In order to view the entire outline of the neuron instead of just the Golgi identified by the Golgi marker, I used mCD8-RFP. This marker is quite useful because mCD8 is a little piece of a mammalian protein that is hooked up to RFP. It will localize mostly to the plasma membrane but will also be found in internal cellular membranes. Thus, it can be used to outline the cells so that I can tell where in the neurons the Golgi appear.

RESULTS

GRASP65-GFP:

In order to see what was going on with the Golgi in both the lva RNAi and the GRIP fusions, I wanted a Golgi marker. Thus, I initially used GRASP65-GFP, which is a Golgi protein in the peripheral membrane that is involved in cisternal stacking (Barr et al., 1997). I used this GRASP65 line to mark Golgi in crosses to lva RNAi, GRIP22 lines, and several yw flies as controls. As shown in Table 3, the numbers of Golgi that I observed in these crosses varied greatly in an apparently random manner. However, the most unexpected observation was that I was seeing Golgi outposts in the axons (Figure 14) even though Golgi outposts have only ever been reported in *Drosophila* dendrites. This was disturbing and suggested that this protein was not actually showing true Golgi or that the expression of the GRASP65-GFP was changing the distribution of Golgi in the flies. I was thus interested in the 2005 Horton et al. paper which reported that overexpression of GRASP65 can disrupt the Golgi. I presumed that this might be the cause of the Golgi I was observing in the axon and decided to look for another Golgi marker to use.

Table 3: This table includes the average number of Golgi seen in the dendrites as well as the percent of the dendritic Golgi that were in branch points for each of the crosses in order to show the variability between crosses.

Averages			
Cross	n (number of larvae)	Average dendritic Golgi per field (±SEM)	Percent dendritic Golgi in branch points (±SEM)
yw x UAS-Grasp65-GFP;elavGal4,UAS-dicer2	4	8.25 ± 1.03	63.6% ± 6.21%
lva RNAi x UAS-Grasp65-GFP;elavGal4,UAS-dicer2	7	6.86 ± 1.55	81.2% ± 13.1%
V.8 Grip 22 on 2 x UAS-Grasp65-GFP;elavGal4,UAS-dicer2	5	12.8 ± 3.06	37.5% ± 6.65%

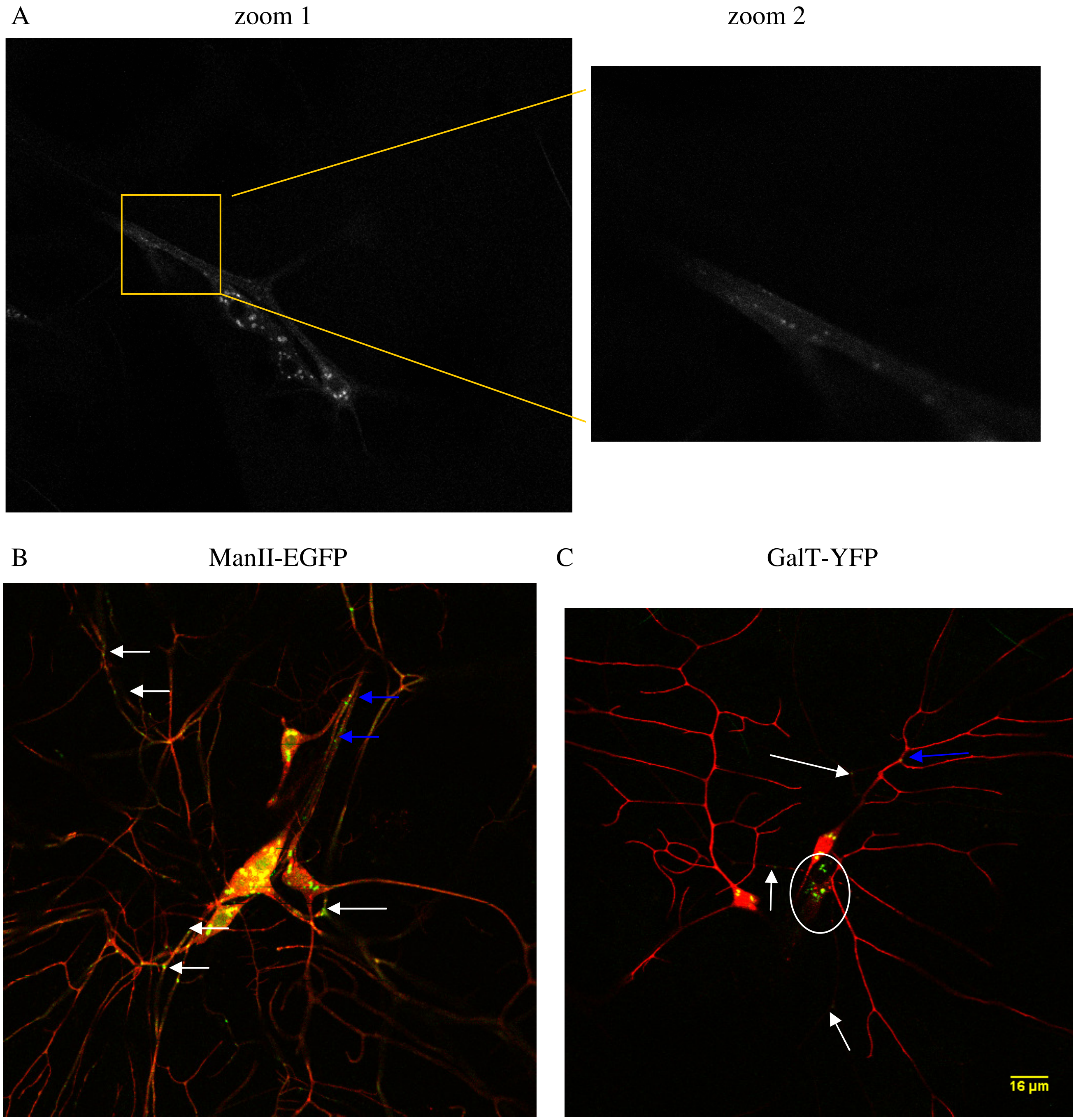

Figure 14: Comparison of Golgi markers
(A) This is an image from a control using GRASP65-GFP with elavGal4. The overview shows the Golgi visible within the cell bodies of the neurons and the enlarged view shows Golgi in the axons. All of the fluorescence that can be seen in the image is GRASP65-GFP.
(B) This was a da neuron cluster from the UAS-mCD8-RFP × 109(2)80,UAS-ManII-EGFP cross. It shows many Golgi throughout the cluster, including some in the axons, some of which are marked by arrows. The blue arrows point to Golgi in the axons and the white arrows point to Golgi in the dendrites. The red is mCD8. The green is ManII-EGFP (Golgi marker).
(C) This image is from a UAS-mCD8-RFP × UAS-GalT-YFP,221Gal4 cross and it shows much

less GFP signal total. The circle is around the class IV da neuron and the other two neurons are class I. The white arrows show Golgi in the class IV neuron and the blue arrow shows the only really visible Golgi in the class I neurons.

ManII-GFP:

After deciding to stop using GRASP65, I found that ManII-EGFP was another possible Golgi marker that had been previously used to mark Golgi outposts in *Drosophila* dendrites (Ye et al., 2007). ManII stands for α-mannosidase II and this protein labels the medial and trans Golgi (Ye et al., 2007). I evaluated the effectiveness of this Golgi marker using the 109(2)80,UAS-ManII-EGFP line crossed to mCD8-RFP. Based on the data obtained with ManII-EGFP (Figure 15), I was seeing some Golgi in the axons and so I decided to focus on using the last Golgi marker, GalT-YFP.

GalT-YFP:

While testing the ManII, I also looked at another Golgi marker used in the 2007 Ye et al. paper, GalT-YFP. This protein is β-1,4-galactosyltransferase, a trans-Golgi protein (Martinez et al., 1997), which is hooked up to EYFP. Although this marker is using YFP rather than GFP as its fluorophore, the fluorescence should be actually brighter than most standard GFP variants (Cubitt et al., 1999) With this GalT-YFP marker, I began by looking at several crosses to GRIP lines rather than controls. After initial examinations of these images, the GalT-YFP marker seemed to show few Golgi in the axons (Figure 14), which was a good indication that it was probably marking true Golgi. Thus, the GalT marker was used for the rest of my imaging experiments.

DISCUSSION

Some of the images taken with GRASP65-GFP show significant GFP signal in distinct puncta in the axons (Figure 14), suggesting that these are Golgi or small pieces of Golgi. As I was imaging, I wondered whether they might be something other than Golgi that the GRASP-65 was binding. However, after seeing the 2005 Horton et al. paper stating that overexpression of GRASP65 changed the organization of the Golgi, I wondered if the GRASP65 could be fragmenting the Golgi and allowing it to pass into the axon. I do not know why it would then be able to pass the diffusion barrier into the axon initial segment, but it seems likely that it did when looking at my images. For the ManII-EGFP, it also seemed as if the protein could be fragmenting the Golgi, since I was seeing Golgi in the axons. I found that it was much more difficult to find a good Golgi marker that would show me the Golgi without interfering with the proper organization of the Golgi than I had anticipated. However, after looking at the GalT-YFP marker, it seemed to have the least amount of Golgi expressing in the axons and I decided that it was probably the most accurate Golgi marker that I had. Thus, I used the GalT for future imaging experiments.

CHAPTER 3: WHERE DO I SEE GOLGI LOCALIZED IN THE FUSION LINES?

Using the most accurate Golgi marker, I wanted to determine whether the kinesin/Golgi fusion could be used to move the Golgi out of dendrites. I was not sure how the fusions would work or where the Golgi would end up. They could be moved into the soma or some of them could be moved out into the axons. I also wanted to know whether all of the Golgi would be moved or if some of them would remain in the dendrites. Thus, I wanted to compare the overall dendritic Golgi distribution in the fusion lines to controls.

To look at the Golgi, I used drivers that express in only class I or class IV da neurons. These da neurons are very useful for imaging on a confocal because they are sensory neurons that reside right below the larval cuticle. Thus, they are close to the surface of the larva and can be easily imaged through their whole depth. There are four classes of these neurons (I, II, III, and IV). The class I da neurons are the simplest and there are two of them in each neuronal cluster.

RESULTS

Class I neurons:

Initially with the GalT-YFP marker, I was using 221Gal4, which is a driver that only expresses in class I da neurons. This makes it very easy to visualize the whole class I neuron with all of its processes. With these crosses, I looked at examples of four GRIP22 and GRIP26 lines containing the transgene on the third chromosome, but I mainly imaged a GRIP22 V.3 line and a control containing no GRIP transgene (Table 4 and Figure 15). The total numbers of dendritic Golgi from the control and GRIP22 V.3 lines did not differ by a statistically significant amount ($p = 0.095$), even though it looked like there was a slightly higher number of Golgi in the

GRIP22 V.3 line. However, I saw few total Golgi outposts in the class I neurons to begin with. It looked as if there was a difference between the proportion of Golgi in branch points versus those outside of branch points in the fusion line as compared to the control. However, an unpaired t-test for this data showed that there was not a statistically significant difference (p = 0.157). The 221Gal4 line also faintly expresses the class IV da neuron, which allowed me to directly compare the class I and IV neurons. Although I was not necessarily seeing all of the Golgi in the class IV neurons since the expression level was lower, it was clear that there were more Golgi in the class IV neurons than in the class I neurons for both the control and GRIP lines.

Table 4: This table shows the average numbers of Golgi in class I and class IV neurons and the fraction of Golgi in branch points as well as Golgi in axons for both a control and experimental cross with the GRIP22 fusion using GalT-YFP to image the Golgi.

	UAS-mCD8-RFP x UAS-GalT-YFP,221-Gal4 (n=20 images, so 40 class I neurons)	UAS-mCD8-RFP;GRIP22 V.3 x UAS-GalT-YFP,221-Gal4 (n=30 images, so 60 class I neurons)
Average dendritic Golgi per class I neuron (±SEM)	1.30 ± 0.183	1.00 ± 0.138
Fraction of Golgi in branch points	0.827 ± 0.0632	0.683 ± 0.0628
Fraction of Golgi not in branch points	0.173 ± 0.0632	0.317 ± 0.0628
Golgi in axons	Only 1 in all 20	Only 1 in all 30 neurons
Average dendritic Golgi visible per class IV neuron (±SEM)	3.30 ± 0.448	3.37 ± 0.481

A control GRIP22 V.3

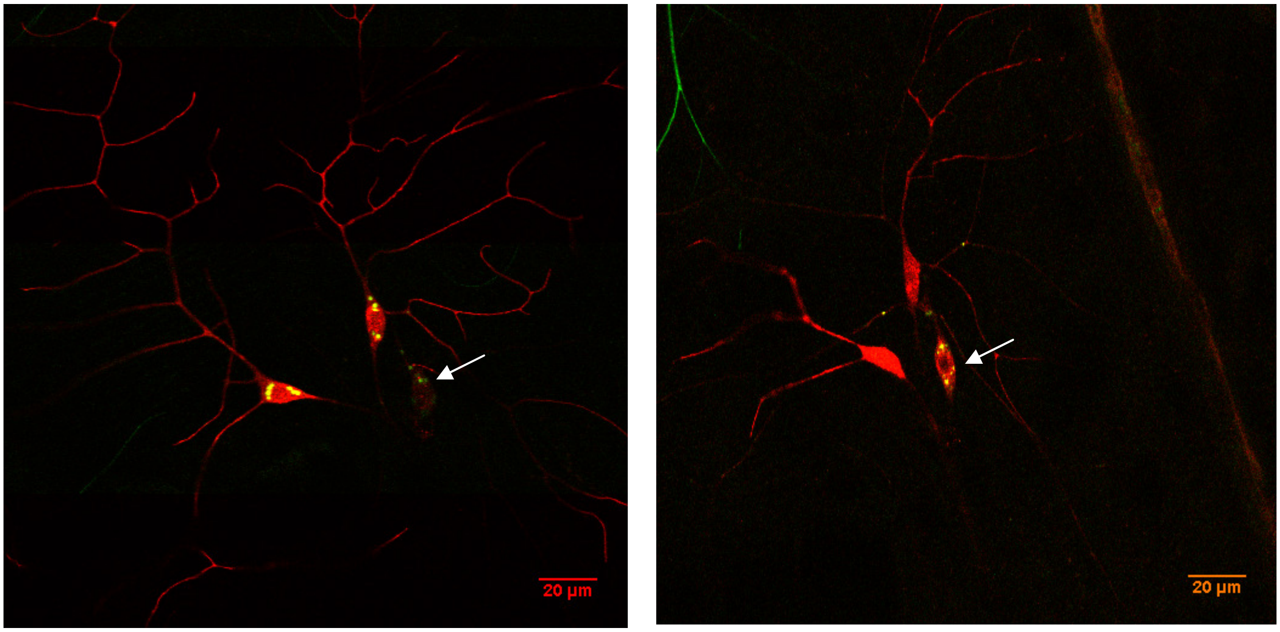

B GRIP22 V.3 C small Golgi in dendrites

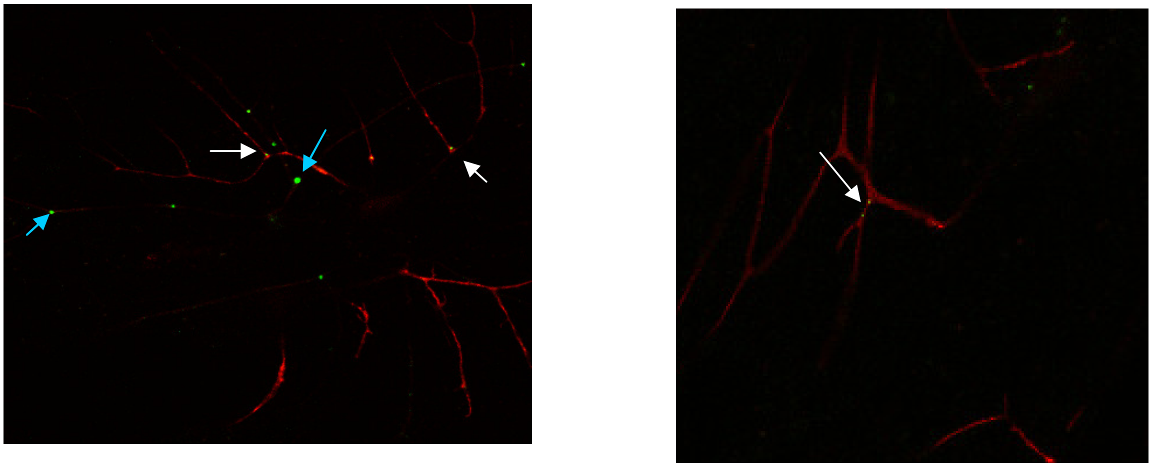

Figure 15: Imaging Golgi using 221Gal4
The red is mCD8-RFP and the green is GalT-YFP, marking Golgi.
(A) The left image is a control of the UAS-mCD8-RFP × UAS-GalT-YFP,221Gal4 cross and the right is an image from a UAS-mCD8-RFP;GRIP22 V.3 × UAS-GalT-YFP,221Gal4 cross. The arrows in both images point to the class IV neuron with the 221Gal4 driver. The dendritic arbors of the class I neurons fan out into comb-like shapes at the tops of the images while not much of the axons are visible but they are pointed down and towards the right of the images.
(B) This is one frame from a time series of images of two class I neurons. The white arrows point to the only two Golgi in the class I neurons, while the blue arrows point to several examples of multiple Golgi in the class IV neuron.
(C) This image shows several “small” Golgi in the dendrites of a class I control neuron which are on either side of the arrow.

Class IV neurons:

The 477-Gal4 driver expresses mainly in class IV da neurons and thus allowed me to look at Golgi directly in class IV neurons. I looked at multiple GRIP lines with the transgene on the third chromosome with the general cross of 477-Gal4;UAS-GalT-YFP × UAS-mCD8-RFP;GRIP line. The control cross was 477-Gal4;UAS-GalT-YFP × UAS-mCD8-RFP. I had the most transgenic data from the GRIP26 JJ.2 cross, but also had data from GRIP26 JJ.5 and GRIP22 V.3 lines. The GRIP26 JJ.2 line was seen to have very low expression of the fusion protein after myc antibody staining, so it is probably not expressing the fusion. The data obtained from the images is recorded in Table 5 and shown in Figure 16.

Table 5: This is the summary of the data from imaging the Golgi in class IV neurons using GRIP26 JJ.2, GRIP26 JJ.5, GRIP22 V.3, and control crosses.

	UAS-mCD8-RFP x 477-Gal4;UAS-GalT-YFP (n=21 neurons)	UAS-mCD8-RFP;GRIP26 JJ.2 x 477-Gal4;UAS-GalT-YFP (n=18 neurons)	UAS-mCD8-RFP;GRIP26 JJ.5 x 477-Gal4;UAS-GalT-YFP (n=9 neurons)	UAS-mCD8-RFP;GRIP22 V.3 x 477-Gal4;UAS-GalT-YFP (n=8 neurons)
Average Golgi per class IV neuron (±SEM)	8.86 ± 0.656	10.3 ± 0.824	5.78 ± 1.02	3.88 ± 0.441
Fraction of Golgi in branch points (±SEM)	0.683 ± 0.0354	0.584 ± 0.0398	0.346 ± 0.0555	0.387 ± 0.121
Fraction of Golgi not in branch points (±SEM)	0.317 ± 0.0354	0.416 ± 0.0398	0.654 ± 0.0555	0.613 ± 0.121
Average Golgi in axons (±SEM)	0.571 ± 0.202	0.556 ± 0.218	3.22 ± 1.05	1.00 ± 0.567

According to Student's unpaired t-test, the difference in number of Golgi between the GRIP26 JJ.2 and control line was not statistically significant ($p = 0.164$). However, the numbers of Golgi in both the GRIP26 JJ.5 and GRIP22 V.3 lines compared to the control were significant ($p = 0.00816$ and $p = 5.78e^{-5}$, respectively). As with the class I neuron images, I also looked at the ratios of Golgi in branch points to those not in branch points. Again it appeared that there was a lower percentage of Golgi in the GRIP lines that were in the branch points than in the control, especially in the GRIP26 JJ.5 and GRIP22 V.3 lines. According to unpaired t-tests performed using the proportions of total Golgi in the branch points, the difference was significant for all three of the GRIP lines ($p = 0.0420$ for GRIP26 JJ.2, $p = 2.27e^{-6}$ for GRIP26 JJ.5, and $p = 6.89e^{-4}$ for GRIP22 V.3).

As another way to analyze the data, I also measured the distances of the Golgi from the soma and the distances to the ends of some of the dendrites as far as I could see them. I compared the proportion of the distances to the Golgi with the total dendrites lengths in several neurons (Table 6). There are fairly few measurements, but the difference in proportions of Golgi are different between the control and GRIP22 V.3 lines according to an unpaired t-test ($p = 0.00572$). Unpaired t-tests for average distances to the ends of the dendrites also show significant differences for both the GRIP22 V.3 and GRIP26 JJ.5 lines ($p = 3.84e^{-6}$ and $p = 4.71e^{-5}$, respectively).

Table 6: This table shows the measurements of Golgi and dendrite tips from the soma with the proportion of Golgi distance to dendritic arbor size in the GRIP fusion lines and control.

	UAS-mCD8-RFP x 477-Gal4;UAS-GalT-YFP (n=5 neurons)	UAS-mCD8-RFP;GRIP26 JJ.2 x 477-Gal4;UAS-GalT-YFP (n=4 neurons)	UAS-mCD8-RFP;GRIP26 JJ.5 x 477-Gal4;UAS-GalT-YFP (n=4 neurons)	UAS-mCD8-RFP;GRIP22 V.3 x 477-Gal4;UAS-GalT-YFP (n=4 neurons)
Average distance to Golgi (µm)	57.7	55.7	21.5	48.8
Average distance to ends of dendrites (µm)	201	154	94.2	111
Proportion	0.287	0.363	0.229	0.441

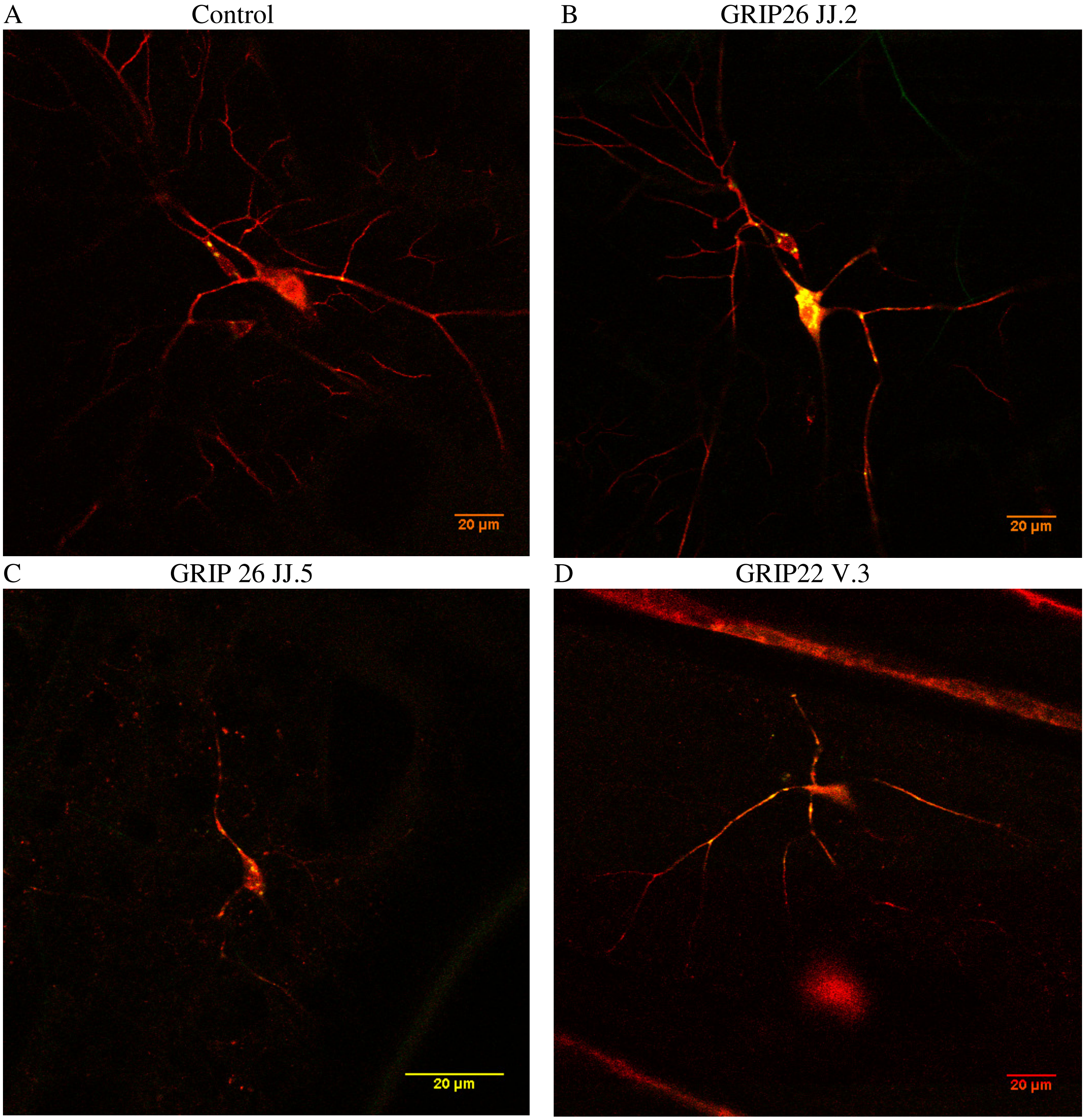
A Control

B GRIP26 JJ.2

C GRIP 26 JJ.5

D GRIP22 V.3

Figure 16: 477-Gal4 images of Golgi using GalT marker in class IV da neurons
In all images, the green is GalT-YFP and the red is mCD8-RFP. The neurons are oriented so that the axon would be pointed down if it were visible in this representative frame and the dendrites are generally oriented up. The control and GRIP26 JJ.2 images also contain class I neurons that the 477-Gal7 driver will also sometimes drive expression in.

A. This is a class IV neuron from a control cross not containing a GRIP fusion.

B. This image is an example of a GRIP26 JJ.2 neuron.

C. This is a GRIP26 JJ.5 neuron that seems to be smaller than the other examples.

D. This is a GRIP22 V.3 neuron that seems to be expressing fairly low levels of mCD8-RFP and seems to have a less extensive dendritic arbor.

DISCUSSION

Class I neurons:

After finding that GalT-YFP seemed to be the most reliable Golgi marker that did not show many Golgi in the axons, which hopefully meant that the expression of the GalT did not disrupt the Golgi distribution, I looked at many neurons using this marker and got definitive data about the Golgi distribution. I did not see the inconsistencies that I saw with the GRASP65 line, although the GRASP65 analysis was with relatively few neurons total. However, I did have trouble coming up with a method to use to count the Golgi and the method I did use was fairly subjective. Since the large, round Golgi most often appearing in branch points were clearly Golgi, I decided to only count these large Golgi. However, there were often also smaller points of GFP that were visible throughout the dendrites. It was sometimes difficult to draw a cut-off as to what was small and what was large in the same image. And it was especially difficult to avoid counting the small Golgi in images where there were no large Golgi in the dendrites. These small fragments of GFP could be Golgi proteins that are not associated with full Golgi outposts. This could be significant because it is possible that the kinesin/Golgi fusions would actually pull a part of the Golgi off and drag it to the soma and leave part of the Golgi behind, which would look like a small Golgi such as I saw. When analyzing these images, I did not look for any difference in numbers of small Golgi between the GRIP and control lines, which would be something that would be interesting to go back and do. However, it would probably be more useful to look at the 477 images since they have more Golgi overall and also larger Golgi, so it would be easier to see a difference.

The GRIP fusion line that I mostly analyzed for the class I da neurons was GRIP22 V.3, which was not a line that I dissected and stained with myc. Thus, I do not have data on whether the fusions are being expressed in this line. It would be very helpful to know information about the expression of GRIP22 in this line in order to know whether I would expect to see a difference in the Golgi distribution in the neurons. Since I did not see a difference in the numbers of Golgi in the dendrites between the GRIP22 V.3 line and the control, it seems likely that this line is not actually expressing the fusion. However, it would be helpful to go back and stain the line with myc to look at the expression.

The most interesting part of these images was being able to compare class I and class IV da neurons since the 221Gal4 driver expresses very lightly in the class IV neuron. Thus, the whole outline of the class IV neuron was not usually visible, but some of the Golgi often were. One observation from comparing the class I and class IV neurons was that the Golgi outposts in class I neurons were noticeably smaller than those in class IV neurons. This makes sense since the class IV neurons are bigger altogether. From looking at both types of neurons together, it was also fairly obvious that there were more Golgi in the class IV neurons. I would often see only one or two big Golgi outposts or even no Golgi outposts in the class I neurons, while there might be five I could see in the class IV neuron, which was at lower levels of expression. Since the class IV neurons are bigger, it makes sense that they would contain more Golgi. However, the fact that there are so few Golgi outposts in the class I neurons suggests that the outposts must not be needed for microtubule polarity in dendrites. Since the class I neurons are relatively small, it may be possible that many Golgi are not needed out in the dendrites for growth of the dendritic arbor. However, if these Golgi were nucleating microtubules in the dendrites, one would expect that the dendrites would need more than one or two Golgi outposts. Thus, it seems as though my hypothesis about the Golgi being necessary for microtubule nucleation may not be correct.

Class IV neurons:

Once I discovered how many more Golgi there were in the class IV neurons, I thought that these would be better neurons in which to evaluate the effects of depleting the Golgi with the GRIP fusions. Thus, I switched to using the 477 driver. The GRIP26 JJ.2 line actually seemed to show more Golgi in the dendrites, although this was not statistically significant. However, the other two lines showed statistically significant decreases in the total number of Golgi in the dendrites. This was quite interesting and showed that the fusion proteins did seem to be working to move the Golgi out of dendrites in the GRIP26 JJ.5 and GRIP22 V.3 lines, but not the GRIP26 JJ.2 line. This makes sense since I did not see much expression of the GRIP26 JJ.2 fusion when I dissected and stained larval filets with myc antibody. Thus, if GRIP26 JJ.2 is not expressing the fusion, it would be expected to have the same Golgi distribution as the control. However, the two fusions that were moving the Golgi did not move all of the Golgi out of the dendrites but only approximately half of the large Golgi. Just from a qualitative assessment of the images as I went through them, there seemed to be a higher number of these lines with the tiny spots of GFP showing up, suggesting that the Golgi were being pulled apart and some Golgi proteins were still being transported out into the dendrites. However, I did not try to quantify this phenomenon in any way. Another interesting observation was that there seemed to be higher numbers of Golgi seen in the axons in some of these GRIP lines, especially the GRIP26 JJ.5 line where there was an average of 3.2 Golgi in the axons. This was pretty variable among the neurons imaged, with one neuron that had 10 Golgi in the axon. However, all but one of the GRIP26 JJ.5 neurons imaged had at least one Golgi in the axon, so there does seem to be a higher proportion of Golgi consistently getting into the axons, even if the numbers vary somewhat. In many of the GRIP neurons imaged, I also saw more moving spots of GFP than I had seen in the controls or GRIP26

JJ.2 line. I would expect that the moving Golgi would probably be vesicles containing Golgi proteins. The movement I saw seemed to be both towards and away from the soma. It is possible that the neurons are trying to get these proteins out into the dendrites because they need the Golgi outposts to process proteins for both intracellular and intercellular signaling. However, I could also be noticing the movement more because there are fewer high-expressing Golgi out in the dendrites in these lines.

Based on the very little measurement data I have from four neurons of each of the GRIP22 V.3 and GRIP26 JJ.5 lines, it looks as if these neurons may have less expansive dendritic arbors. This could reflect a need for the Golgi outposts in dendrites in order for the dendrites to grow far from the soma. However, the small sample sizes do not constitute enough data to show any true trend. For the GRIP22 V.3 neurons, it looks as if the Golgi outposts were farther from the edges of the dendrites, which could be possible if they are about the same distance from the soma but the dendritic arbor is smaller. For the GRIP26 JJ.5 measurement data, the proportion is fairly similar to that of the control, suggesting that the Golgi are the same distance proportionally from the cell body although those dendritic arbors may be smaller.

I do have fewer total neurons of the GRIP22 V.3 and GRIP26 JJ.5 lines than the control or GRIP26 JJ.2 lines. This raises the question of whether they are large enough samples from which to draw any conclusions. It would be nice to have some more data from these lines even though I was able to show statistically significant results with the data I do have. With the GRIP22 V.3 line, I have 8 neurons and with the GRIP26 JJ.5 line I have 9 neurons. Based on previous research in the lab using this live larval microscopy, ten to twenty neurons has been a large enough sample size to see phenotypes. In a recently published paper, sample sizes of neurons ranged from five to fifteen and statistically significant results were seen in these samples

(Stone et al., 2010). Thus, my sample sizes for the GRIP26 JJ.5 and GRIP22 V.3 lines are at a size I would expect to be significant, especially since they seemed to reveal a fairly significant phenotype in its difference from the control.

In all of the GRIP lines, including GRIP26 JJ.2, there was a significantly lower proportion of Golgi in dendritic branch points than in the control. This is a fairly interesting phenotype that is not necessarily expected. It is possible that the GRIP fusions are causing the Golgi outposts to be less tightly tethered to the branch points and more likely to be in the middle of branches. It is also possible that the Golgi are being pulled partway towards the soma. To know if this were the case, it would be helpful to have more measurement data to see if the Golgi in the fusions tend to be closer to the soma. Another consideration is the size of the Golgi remaining in the dendrites. Perhaps Golgi tend to localize to branch points because that is where they fit best and when the Golgi are smaller, more of them will end up in the middle of the branches.

It is interesting to me that the GRIP22 V.3 line did not seem to cause any significant phenotype in the class I neurons. If there was any phenotype in the class I da neurons, it seemed to be an increase in the number of Golgi in the dendrites. However, this difference was not statistically significant since the total number of Golgi is so much smaller in the class I neurons. Similar to the class IV phenotype, the line seemed to show a decrease in the Golgi at branch points in the class I neurons, which was again not significant, probably because there are few total Golgi. It seems odd that I did not see a decrease in the number of dendritic Golgi in the class I da neurons and it may suggest that a certain number of Golgi are required in the dendrites for survival. However, this may not be the case since there were class I neurons that contained no large dendritic Golgi and seemed to be fully functional. Comparing the percentages of Golgi in the branch points between class I neurons with the 221 driver and class IV neurons with the 477 driver in the controls is also interesting. There were lower percentages overall of Golgi in the branch points of the class IV neurons, meaning that there were more Golgi residing in between branch points. This could just be a result of having more dendritic Golgi in these neurons. It could also be a result of the dendrites being larger and thus containing more room for Golgi outposts throughout the dendrite as well as in branch points.

Now that I have looked at the Golgi distribution in the GRIP fusions and have seen differences from the control in the GRIP26 JJ.5 and GRIP22 V.3 lines, I would like to use EB1-GFP to look at the microtubule dynamics in these lines. Since a significant number of Golgi seem to have been removed from these lines, it will be interesting to see if there is a change in microtubule dynamics in these lines. This will show whether the Golgi are actually nucleating microtubules in the dendrites.

CHAPTER 4: WHAT CAN I DISCOVER USING AN ALTERNATE METHOD TO DEPLETE THE GOLGI?

In addition to the GRIP fusions, I wanted to use another technique to deplete Golgi and look for a phenotype. To do this, I used RNAi for lava lamp (lva), a Golgi-associated protein. This technique works by introducing a short hairpin of double-stranded RNA into the cell. When dsRNA is present, the cell destroys it because it may a sign of an invading virus. Because the dsRNA is homologous to the lva transcript, the cells where it is introduced will delete all lva RNA. Thus, there will be much less lva in the animal. In flies, RNAi is much more effective when exogenous Dicer2 protein is added because this extra protein will process the hairpin RNA into siRNA which will then help knock down the activity of the endogenous lva protein. Thus, I included a fly line containing a UAS-dicer2 construct in my genetics for lva RNAi.

Lva is involved in the interactions between Golgi and the dynein/dynactin complex (Papoulas et al., 2005). Since dynein is required for positioning the Golgi, depleting lva should change the distribution of Golgi in the neuron. When Lva RNAi was used previously in neurons by Ye et al. (2007), they saw that it did change the distribution of Golgi and seemed to decrease the size and number of Golgi outposts in dendrites. This also decreased the branching and complexity of the dendritic arbor. Based on my hypothesis, I thought that the phenotypes observed by Ye et al. from the depletion of Golgi might be explained by the dendritic Golgi being needed to nucleate microtubules. Thus, I wanted to look at microtubule dynamics in these neurons to see if the depletion in Golgi would change the polarity of microtubules if they were losing their dendritic nucleation sites.

To evaluate the microtubule dynamics, I used the protein EB1, which binds to plus ends of microtubules. Thus, the EB1 will track along growing microtubules, which reveals the direction in which the microtubules are growing. This EB1 protein is attached to a GFP so that it will fluoresce and can be visualized by microscopy. This technique allowed me to determine whether or not the Golgi were affecting the polarity of the microtubules.

RESULTS

For imaging the RNAi lines, fairly large 3rd instar larvae were used that had developed for four days after the eggs were laid. Older larvae were desired because the RNAi would have had more time to knock down its target protein. However, older larvae were also harder to hold still enough to collect useful images of the moving EB1 comets. Thus, I used several different methods to hold the larvae still as they were being imaged including a mixture of chloroform and halocarbon oil to knock out the larvae and agarose slides to pull moisture out of the larval cuticle and hold the larvae in place. For most of these larvae, I was imaging in the 4th, 5th, or 6th hemisegments, near the middle of the larvae. First an overview was taken of the neuron cluster and then I zoomed in on the class I neuron to look at the microtubule dynamics. These images were analyzed by counting the numbers of EB1 comets going in each direction, both towards the soma and away from the soma. The comets were counted if they were visible for at least three frames in a row and if they were in the main trunk of the neuron rather than a branch off of the main trunk. From this analysis, I found the results shown in Table 7. For the control, ncd RNAi, I looked at neurons from 20 larvae, but for the lva RNAi I had a smaller sample with neurons from only 8 larvae (1 neuron per larva). I had originally taken more lva RNAi images but several were unusable because the larva had died and there was no EB1 activity or I had mistakenly imaged neurons that were not class I da’s. These images were collected when I was first learning to use the microscope to image larvae, so the image quality was sometimes poor, and it is unfortunate that I did not get a few more usable lva images. However, the data that I did get showed a very similar result for both ncd and lva RNAi.

Table 7: This is data from the images of neurons from larvae of ncd and lva RNAi crosses.

RNAi imaging results for ncd RNAi (control) and lva RNAi			
UAS-EB1-GFP,109(2)80;UAS-dicer2 × ncd RNAi n = 20 larvae	Towards soma	Away from soma	Total
Number of comets	136	22	158
Percentage	86.1	13.9	100
UAS-EB1-GFP,109(2)80;UAS-dicer2 × lva RNAi n = 8 larvae	Towards soma	Away from soma	Total
Number of comets	71	13	84
Percentage	84.5	15.5	100

This data does not appear to reveal a significant difference between lva and ncd, and a chi-square test with this data confirmed that there was no statistically significant difference. Previous research in the Rolls lab had shown about 94% minus end out microtubules in dendrites proximal to the soma (Stone et al., 2008). This was with the driver elav-Gal4, which expresses less intensely than the 109(2)80 driver. When EB1 is overexpressed, it can change the microtubule dynamics. Thus, using the 109(2)80 driver could be the cause of the less polarized microtubule array observed in the control data calculated here with ncd RNAi. Other people in the lab have seen about 90% of microtubules minus end out with the 109(2)80 driver. The observed 86% of microtubules growing towards the soma is reasonably close to 90% and since there was very little difference between the control and lva RNAi (84.5%), it seems clear that the depletion of lva RNAi did not affect microtubule polarity. As a positive control to make sure that the RNAi was working to knock down the protein, I set up a cross of the 109(2)80,UAS-EB1-GFP;UAS-dicer2 line to EB1 RNAi and saw no EB1 expression (no GFP fluorescence). This was important because it told me that the dicer2 was helping to fully knock down the RNAi and thus the other RNAi lines I was using should also have their respective proteins knocked down.

DISCUSSION

I originally wanted to look at the effect of lva RNAi because of the 2007 Ye et al. paper where they saw that lva RNAi reduced the size of Golgi outposts in *Drosophila* class IV da dendrites and also caused less branching in the dendritic arbor. This made me think that the decrease in branching could be due to the decrease in Golgi outposts. It makes sense that the Golgi would be necessary to process proteins out in the dendrites for growth and that a reduction in Golgi would lead to less growth whether or not the Golgi were also involved in nucleating microtubules. However, I wanted to see whether the decrease in dendritic Golgi outposts had any effect on microtubule polarity. Based on the data I collected, it does not seem that the reduction of Golgi through lva RNAi has an effect on microtubule polarity. But there are several ways in which this experiment could have been conducted more conclusively. It would have been nice to have data from a few more larva expressing lva RNAi to compare to the control. Also, my choice of control was not necessarily something guaranteed to have no phenotype. The protein ncd is a minus-end directed kinesin and although I had not noticed any phenotype from depleting it at the time I used it as a control, it seems very likely to be related to microtubule dynamics. Later on, the lab began to use reticulon2 (rtln2) RNAi as a control. These larvae were held still while being imaged using chloroform, which could have deleterious effects on the larvae at certain levels. Although I used this method for a while and the microtubule dynamics did seem normal, it could have been the suboptimal conditions for the larvae.

It would also be interesting to look at the Golgi in the lva RNAi neurons. Based on my imaging with the UAS-GalT-YFP Golgi marker in class I da neurons, there seem to be few dendritic Golgi outposts. Thus, there might not be much effect on the dendritic arbor of class I neurons if the reduction in Golgi is what caused the reduction in branching seen in the 2007 Ye et al. paper. This is something that it would be interesting to go back and evaluate in my images. It would also be interesting to look at the class IV neurons with the GalT-YFP marker and lva RNAi to see the effect of depleting lva on the Golgi. This would show whether there is a difference in Golgi distribution with the lva RNAi and if I am reproducing the phenotype observed in the Ye et al. paper. I could also compare the effects of lva RNAi on the Golgi to the Golgi distribution seen in the GRIP fusions.

It would also be helpful to evaluate whether the Golgi may be nucleating microtubule minus ends using other methods besides depleting the Golgi. To investigate this, the Rolls lab has looked at the dendritic localization of several microtubule minus end-associated proteins that were attached to GFP constructs and incorporated into the fly genome such as γ-tubulin-GFP. With the γ-tubulin-GFP, we did not see any specific localization points within the dendrites. We are also doing RNAi screens in da neurons with any molecules that are known to be nucleated at the centrosome. Another possible method might be to do a yeast two hybrid screen for proteins in the dendrites that could bind to γ-tubulin to nucleate the microtubule minus ends. A positive control for this screen could be a protein that γ-tubulin is known to bind to in the γ-TuRC such as the various γ-tubulin complex proteins (GCPs) (Raynaud-Messina and Merdes, 2007) or centrosomal proteins. A second approach for looking at the nucleation of microtubules in *Drosophila* dendrites would definitely be useful and possibly one of these methods could yield an answer to the question of dendritic microtubule nucleation.

CONCLUSIONS

Based on the results of my experiments, it appears that the kinesin/Golgi fusion constructs are working to move Golgi out of the dendrites. This was confirmed through antibody staining for to analyze whether the GRIP constructs were being expressed in the *Drosophila* larvae. I did see expression of the constructs in some of the GRIP lines and these lines also contained fewer Golgi in the dendrites based on fluorescence microscopy with a GFP Golgi marker. Future experiments to test the microtubule polarity within the dendrites of the fusion lines will reveal the effect of moving the Golgi on microtubules. However, when imaging the class I da neurons, I saw that there were very few Golgi in the dendrites of these neurons. The average in the wild type class I neurons was 1.30 dendritic Golgi per neuron. Even though wild type class IV neurons contain many more dendritic Golgi outposts, the limited number of dendritic Golgi in the class I da neurons suggests that dendritic Golgi are probably not required for nucleating microtubules. Regardless of this, the kinesin/Golgi fusion approach to moving the Golgi could prove to be very useful in future experiments to characterize the role of the Golgi in dendrites. Since some of the lines showed that Golgi outposts were also moved into axons, these fusions could also be used to evaluate the effect of adding Golgi to these processes. Thus, the kinesin/Golgi fusion technique for moving the Golgi has been proven to work and can now be used for further experiments.

REFERENCES

Adams, C.M., Anderson, M.G., Motto, D.G., Price, M.P., Johnson, W.A., and Welsh, M.J. 1998. Ripped pocket and pickpocket, novel *Drosophila* DEG/ENaC subunits expressed in early development and in mechanosensory neurons. *J Cell Biol*. 140:143-152.

Ahmad, F.J., Yu, W., McNally, F.J., and Baas, P.W. 1999. An essential role for katanin in severing microtubules in the neuron. *J Cell Biol*. 145:305-315.

Arimura, N., and Kaibuchi, K. 2007. Neuronal polarity: from extracellular signals to intracellular mechanisms. *Nat Rev Neurosci*. 8:194-205.

Baas, P.W., Deitch, J.S., Black, M.M., and Banker, G.A. 1988. Polarity orientation of microtubules in hippocampal neurons: uniformity in the axon and nonuniformity in the dendrite. *Proc Natl Acad Sci USA*. 85:8335-9.

Baas, P.W., Karabay, A., and Qiang, L. 2005. Microtubules cut and run. *Trends Cell Biol*. 15:518-524.

Barr, F.A., Puype, M., Vandekerckhove, J., and Warren, G. 1997. GRASP65, a protein involved in the stacking of Golgi cisternae. *Cell*. 91:253-262.

Brady, S.T. 1985. A novel brain ATPase with properties expected for the fast axonal transport motor. *Nature.* 317:73-75.

Burton, P.R., and Paige, J.L. 1981. Polarity of axoplasmic microtubules in the olfactory nerve of the frog. *Proc Natl Acad Sci USA*. 78:3269-73.

Conde, C., and Caceres, A. 2009. Microtubule assembly, organization and dynamics in axons and dendrites. *Nat Rev Neurosci*. 10:319-332.

Craig, A.M., and Banker, G. 1994. Neuronal polarity. *Annu Rev Neurosci*. 17:267-310.

Efimov, A., A. Kharitonov, N. Efimova, J. Loncarek, P.M. Miller, N. Andreyeva, P. Gleeson, N. Galjart, A.R. Maia, I.X. McLeod, J.R. Yates, 3rd, H. Maiato, A. Khodjakov, A. Akhmanova, and Kaverina, I. 2007. Asymmetric CLASP-Dependent Nucleation of Noncentrosomal Microtubules at the trans-Golgi Network. *Dev Cell*. 12:917-30.

Horton, A.C., Racz, B., Monson, E.E., Lin, A.L., Weinberg, R.J., and Ehlers, M.D. 2005. Polarized secretory trafficking directs cargo for asymmetric dendrite growth and morphogenesis. Neuron. 48:757-71.

Kwan, A.C., Dombeck, D.A., and Webb, W.W. 2008. Polarized microtubule arrays in apical dendrites and axons. *Proc Natl Acad Sci USA*. 105:11370-11375.

Marcus, A., Bernhardt, R., and Hugh-Jones, T. 1981. High molecular weight microtubule-associated proteins are preferentially associated with dendritic microtubules in brain. *Proc Natl Acad Sci USA*. 78:3010-3014.

Martinez, O., Antony, C., Pehau-Arnaudet, G., Berger, E.G., Salamero, J., and Goud, B. 1997. GTP-bound forms of rab6 induce the redistribution of Golgi proteins into the endoplasmic reticulum. *Proc Natl Acad Sci*. 94:1828-1823.

McIntosh, J.R., and Euteneuer, U. 1984. Tubulin hooks as probes for microtubule polarity: an analysis of the method and an evaluation of data on microtubule polarity in the mitotic spindle. *J Cell Biol*. 98:525-533.

Mitchison, T., and Kirschner, M. 1984. Dynamic instability of microtubule growth. *Nature*. 312:237-242.

Papoulas, O., Hays, T.S., and Sisson, J.C. 2005. The golgin Lava lamp mediates dynein-based Golgi movement during *Drosophila* cellularization. *Nat Cell Biol.* 7:612-618.

Parton, R.G., Simons, K., and Dotti, C.G. 1992. Axonal and dendritic endocytic pathways in cultured neurons. *J Cell Biol*. 119:123-137.

Raynaud-Messina, B., and Merdes, A. 2007. Gamma-tubulin complexes and microtubule organization. *Curr Opin Cell Biol*. 19:24-30.

Rogers, G.C., N.M. Rusan, M. Peifer, and Rogers, S.L. 2008. A multicomponent assembly pathway contributes to the formation of acentrosomal microtubule arrays in interphase Drosophila cells. *Mol Biol Cell*. 19:3163-78.

Rolls, M.M., Satoh, D., Clyne, P.J., Henner, A.L., Uemura, T., and Doe, C.Q. 2007. Polarity and intracellular compartmentalization of Drosophila neurons. *Neural Dev*. 2:7 (1-14).

Rothwell, J. 2009. Meet the brain: neurophysiology. *Int Rev Neurobiol*. 86:51-65.

Stone, M.C., Nguyen, M.M., Tao, J., Allender, D.L., and Rolls, M.M. 2010. Global up-regulation of microtubule dynamics and polarity reversal during regeneration of an axon from a dendrite. *Mol Biol Cell*. 21:767-777.

Stone, M.C., Roegiers, F., and Rolls, M.M. 2008. Microtubules Have Opposite Orientation in Axons and Dendrites of Drosophila Neurons. *Mol Biol Cell*. 19:4122-4129.

Cubitt, A.B., Woollenweber, L.A., and Heim, R. 1999. Understanding Structure-Function Relationships in the *Aequorea victoria* Green Fluorescent Protein. in *Methods in Cell Biology Volume 58: Green Fluorescent Proteins*. (Sullivan, K.F., and Kay, S.A., Ed.) pp 19-30, Academic Press, San Diego, CA.

Ye, B., Zhang, Y., Song, W., Younger, S.H., Jan, L.Y., and Jan, Y.N. 2007. Growing dendrites and axons differ in their reliance on the secretory pathway. *Cell*. 130:717-29.

ACADEMIC VITA

CHRISTIE McCRACKEN
cjm5128@psu.edu

Current Address:
408 Atherton Hall
University Park, PA 16802
Cell Phone: 412-600-7761

Permanent Address:
107 Sheffield Lane
McMurray, PA 15317
Home Phone: 724-941-7539

EDUCATION

The Pennsylvania State University, State College, PA
Bachelor of Science in Biochemistry and Molecular Biology
Anticipated Graduation: May 2010
Schreyer Honors College Student
Thesis: *Effect of the Golgi on Drosophila Dendritic Microtubule Nucleation*

Dean's List 2006-2009
Member of Phi Beta Kappa

Relevant Courses:
- Organic Chemistry with lab
- Physical Chemistry
- Microbiology with lab
- Physics
- Immunology
- Viral Pathogenesis
- Proteins, Nucleic Acids, and Molecular Cloning Lab
- Protein Purification and Enzymology Lab

RESEARCH EXPERIENCE

Lab of Dr. Melissa Rolls in Penn State BMB department, Researcher
Fall 2007-present
- Mastering manipulative genetics techniques with Drosophila crosses
- Learning techniques for isolating and cloning DNA (gel electrophoresis, polymerase chain reaction, restriction enzyme digests)
- Employing fluorescence microscopy and RNAi live imaging techniques (with larvae)
- Conducting research project manipulating microtubule polarity in Drosophila dendrites
- Dissecting larvae for antibody staining of neurons

HONORS

- Robert C. Byrd Honors Scholarship (2006-2010)
- National Merit Scholarship Corporation Scholarship (2006-2010)
- Whitfield Research Fund Summer Research Award (2008)
- Irving and Jeanne Atlas Scholarship in Biochemistry (2008-2009)
- John Van Valzah Foster, Jr. M.D. and Carlyn Manifold Foster Memorial Scholarship in Biochemistry and Molecular Biology (2009-2010)
- Schreyer Honors College Academic Excellence Scholarship (2006-2010)

EXTRACURRICULAR ACTIVITIES

- Campus Crusade for Christ (2006-2010)
- Sinfonietta Orchestra, violinist (2006-2007, 2009)
- Schreyer Honors College Orientation Mentor (2009)